University of Southern Queensland
Faculty of Health, Engineering & Science

Feasibility Study to Upgrade DOL Driven Pumps to Variable Speed Drives

A dissertation submitted by

Aaron Chambers

In fulfilment of the requirements of

ENG4112 Research Project

towards the degree of

Bachelor of Electrical & Electronic Engineering

Submitted: October, 2021

(Page Left Intentionally Blank)

Abstract

Centrifugal pumps operating at constant speed with the discharge flow throttled consume unnecessary energy. Implementation of variable speed drives can reduce this energy consumption through the reduction of pump speed. The introduction of variable speed drives can also impact other aspects of the equipment and system, including environmental emissions, maintenance requirements and equipment performance which all require consideration.

Effective metrics to measure such a proposal are known as the life cycle cost and payback period analysis. These tools consider all financial impacting aspects of the proposal over either a 12 month period or the operating life of the equipment to determine a projects feasibility. In this application financial impact consideration has been given to energy consumption, environmental emissions, maintenance requirements, motor cooling capacity, system harmonics, cable transmission line effects and equipment purchase, installation and commissioning costs.

Through the above mentioned analysis it can be concluded that significant energy, environmental and maintenance cost benefits are available , equipment operational life impacts are negligible and purchase, installation and commissioning costs are expensive. This results in a large 5.48 million dollar life cycle costs benefit but a long payback period of 3.7 years associated with this proposal.

University of Southern Queensland

Faculty of Health, Engineering & Science

ENG4111 / 2 Research Project

Limitations of Use

Certification of Dissertation

I certify that the ideas, designs and experimental work, results, analyses and conclusions set out in this dissertation are entirely my own effort, except where otherwise indicated and acknowledged.

I further certify that the work is original and has not been previously submitted for assessment in any other course or institution, except where specifically stated.

A. Chambers

[redacted]

Acknowledgments

My wife, Monique for supporting me during the dedication of untold hours to this project while unknowingly neglecting her and my family.

My supervisor, Tony Ahfock for guiding me through this daunting process and keeping me on track when at times I felt lost and overwhelmed.

Completion of this project and dissertation would not have been possible without their contributions. Thankyou both

Table of Contents

List of Figures

List of Tables

Chapter 1

Introduction

1.1 Yara Pilbara Overview

Yara is the leading global producer of fertiliser and provides sustainable solutions to world food production. It has sales and operations all over the world including an ammonia fertiliser plant located on the Burrup Peninsula in Karratha Western Australia illustrated below in figure 1.1.

Figure 1.1 geographic location of the Yara Pilbara Ammonia Fertiliser plant (Where we operate | Yara Australia, 2021)

This plant utilises the well proven Kellogh Braun & Root (KBR) ammonia purification process to extract hydrogen from natural gas and mix it with nitrogen from the air to produce 2450 metric tonnes of liquified anhydrous ammonia per day. The liquified ammonia is then pumped approximately 5km to the port of Dampier where it is loaded onto shipping vessels for transport to national and international customers.

This product is then utilised in further processing plants to produce either ammonium nitrate or urea which can then be mixed with other ingredients such as phosphorous and potassium to produce various versions of high quality fertiliser. High quality fertiliser is a necessity to increase the yield of farming crops and reduce the pressure from a growing population and a reduction in food supply and aligns with the Yara's mission to responsibly feed and protect the world.

1.2 Background and Justification

Ammonia production is a process that consumes large amounts of natural gas in both the processing plant and utilities equipment. Production efficiency is a measure of how much natural gas is consumed in giga joules per tonne of produced liquid anhydrous ammonia and it therefore follows that reducing the consumption of natural gas will reduce greenhouse emissions and increase production efficiency and company profits.

The ammonia production process in figure 1.2 requires several utilities services to support its production and includes sea water, desalinated water, demineralised water, instrument air, process air, nitrogen, steam and electricity. The site electricity is supplied by two parallel connected 20 megawatt (MW) steam turbine generators connected to a varying load of approximately 15MW. The steam supply for these two generators are provided from two fuel gas fired boilers with an operating capacity of 50 tonnes (T) and 150T respectively. It can be said that the production of site electricity is a 2 stage process in which steam is first produced to drive the generator turbine to produce electricity which results in 2 stages of efficiency losses via the water to steam conversion in the boilers and then the steam to electricity losses in the turbine generators.

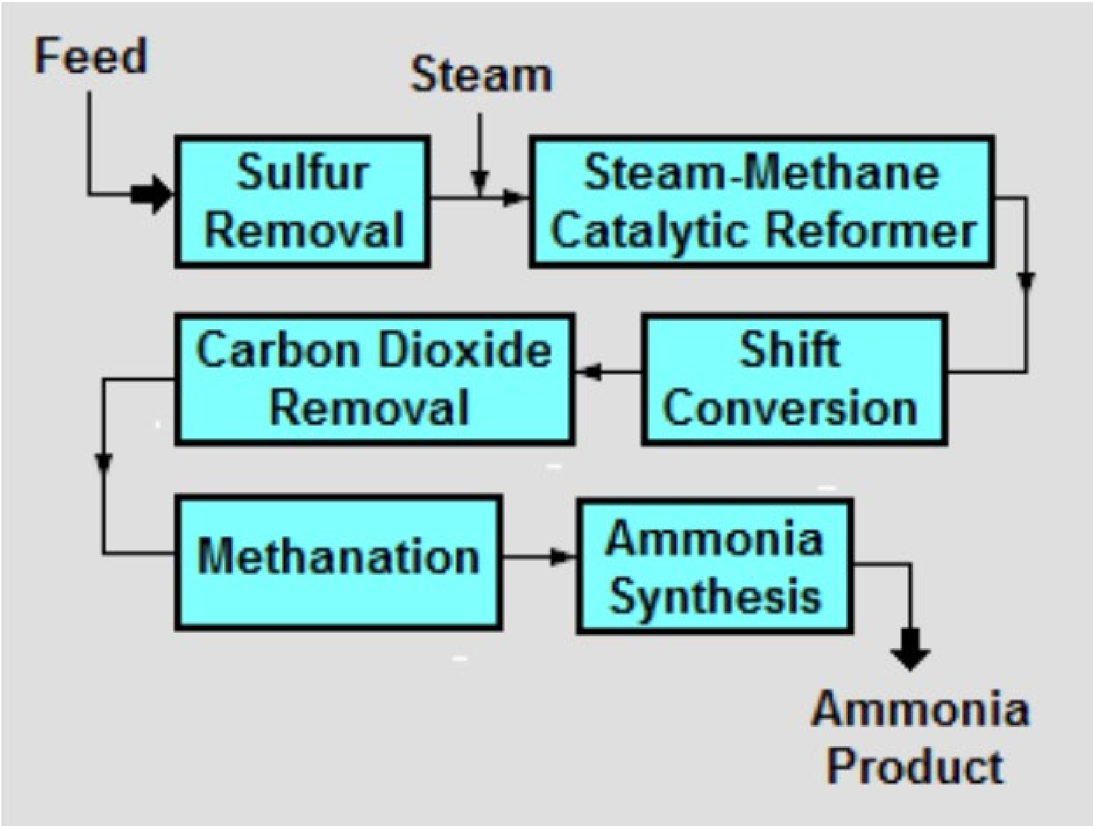

Figure 1.2: Ammonia production block diagram (Ammonia production - Wikipedia, 2021)

It therefore follows that a reduction of electricity consumption will result in a magnified reduction in gas consumption and a significant improvement in plant efficiency.

Within the ammonia utilities plant resides three large centrifugal sea cooling water pumps driven by large 2.7MW constant speed high voltage (HV) motors . These pumps are required to supply cooling water at a pressure of 450 kilopascals (kPa) and 35 degree Celsius to various heat exchangers and condensers throughout the plant with two out of 3 pumps operating in parallel 24 hours a day with a throttled discharge flow into a common header. The configuration of these pumps results in significant consumption of electricity and forms the basis for this research project to conduct a feasibility study to upgrade these motors to operate with variable speed drives (VSD's) and reduce the associated energy consumption to improve overall plant efficiency and greenhouse emissions.

1.3 Project Aims and Objectives

This project aims to conduct a feasibility study of upgrading the existing DOL driven centrifugal pumps currently with throttled discharge flow to VSD driven centrifugal pumps. The following objectives will ensure the project aim is realised.

- Identify life cycle costs associated with both VSD and DOL pumping applications.
- Review the existing hydraulic pumping system to determine and model the system requirements, demand and curves.
- Measure and obtain field data and calculate existing system power consumption and flow output to determine the specific energy of the system.
- Assess the VSD's installation and impact to the existing motors and pumps in terms of efficiency and operating parameters.
- Analyse and calculate the specific energy of the proposed VSD system.
- Review, identify and quantify other associated benefits including maintenance, operations and environmental costs.
- Conduct a cost benefit analysis of the proposed upgrade and determine the payback period.
- Consider alternative options to improve the system. (time permitting)
- Expand the analysis and findings to additional site pumping systems with similar conditions to extrapolate the benefits (time permitting)

Satisfying the above objectives will ensure the system and equipment is analysed in sufficient detail to identify and quantify the life cycle costs associated with both pumping systems. This will lay the foundations to perform the cost benefit analysis and determine the payback period of the proposal.

1.4 Thesis Overview

Chapter 1 introduces the project and provides background and justification for project selection. The project aims and objectives are then discussed which will ensure the project goals can be achieved.

Chapter 2 is a comprehensive literature review researching existing work conducted within the topic area of VSD implementation. This include energy consumption, environmental impact, total harmonic distortion, transmission line effects, thermal analysis, life cycle costs and payback period analysis.

Chapter 3 details the project methodology that will ensure the project goals, aims and objectives are achieved. This includes a large amount of data collection that will allow the analysis, modelling and validation of the proposal to be conducted. These results can then be transferred to the life cycle and payback period analysis.

Chapter 4 analyses the proposal from an energy consumption perspective which involves modelling of both the existing and proposed hydraulic and pumping systems . Additionally pump and VSD efficiency are considered here to determine the energy related cost impact of the proposal.

Chapter 5 continues the analysis and investigates additional proposal impacts other than energy consumption. These include environmental emissions, maintenance requirements, purchase and installation requirements and motor operating life due to harmonic distortion, transmission line effects and thermal analysis. These are then financially quantified for further analysis.

Chapter 6 combines the results from the previous two chapters into a life cycle cost and payback period analysis. Here the financial benefits are concluded over the entire the life cycle of the variable speed drives as well as a metric of how long the proposal will take to pay for itself.

Chapter 7 concludes the research from the earlier chapters and presents further work that could utilise the research, results and findings presented in this from document.

Chapter 2

Literature Review

2.1 Introduction

The intent of this chapter is to research existing relevant literature and determine a pumping drive system upgrade feasibility study methodology that can be applied to the Yara Pilbara Fertilisers site sea cooling water pumping equipment. The research will focus on the below key topics :

- Energy consumption improvements associated with the upgrade from a DOL throttle flow control system to a VSD controlled system.
- Environmental impacts that can be achieved from a reduction in energy consumption.
- Other considerations that contribute to the life cycle costs of the proposed upgrade such as motor insulation and partial discharge and maintenance and operation costs.

Thorough research of the above topics will ensure an accurate life cycle cost benefit and payback period analysis can be conducted and feasibility determined in this particular application. The information gleaned from this research is detailed in the following sections.

2.2 Energy Consumption Improvements

Pumping systems account for nearly 20% of the total world electrical energy demand and range from 25% to 50% of energy consumption in the majority of industrial plants (Ahonen, Pöyhönen, Siimesjärvi and Tolvanen, 2018) and figure 2.1 shows a typical distribution of energy demand in an industrial plant. Energy efficiency improvements provide an opportunity to significantly reduce plant energy consumption with measurable savings.

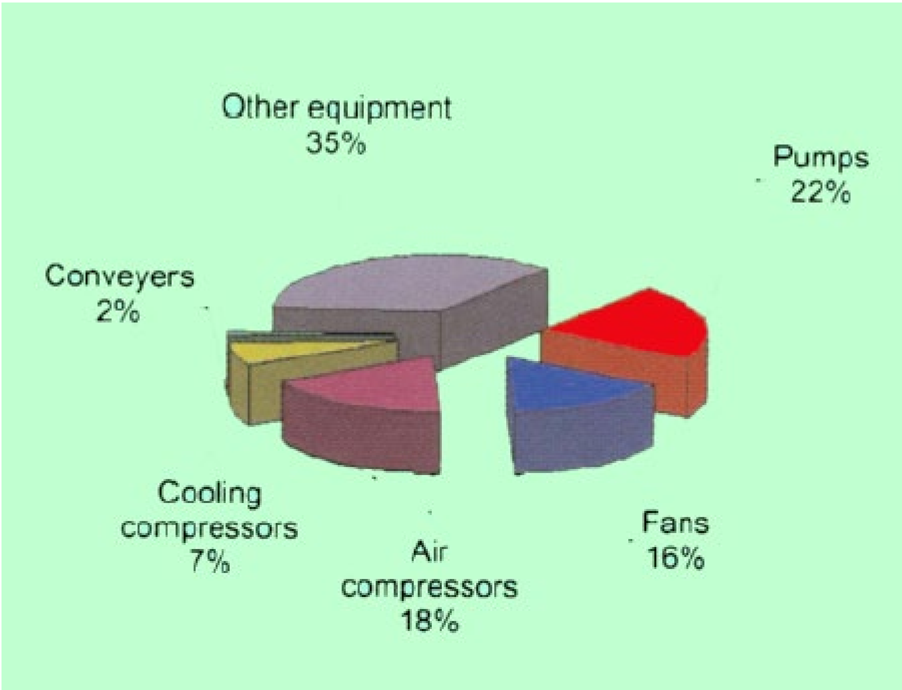

Figure 2.1: Typical industrial plant electrical distribution (Institute, 2004)

A pumping system consists of a motor drive and a pump or pumps that is required to transfer liquid through the hydraulic system. At a minimum the pumping system is designed to ensure that it can deliver the maximum required flow capacity at any given time, however in practice pumps are typically oversized and operate at non optimal speeds resulting in inefficient energy consumption and wasted resources (Ahonen, Pöyhönen, Siimesjärvi and Tolvanen, 2018).

The hydraulic system is the combination of piping, valves, pipe fittings, process equipment and geographic elevation between the pump suction and product destination. This system can be separated into two main components known as the static head and friction loss head. The Static head is the change in elevation between the start and destination point of the system and represents the opposing gravitational force that the liquid must be lifted to overcome (Mackay, 2004). The friction loss on the other hand is the resistance to flow that is introduced in the system by pipes, valves, fittings and other equipment such as heat exchangers or condensers (Mackay, 2004). The static head component is constant in relation to flow while the friction loss head component is a function of the system flow which is illustrated in figure 2.2

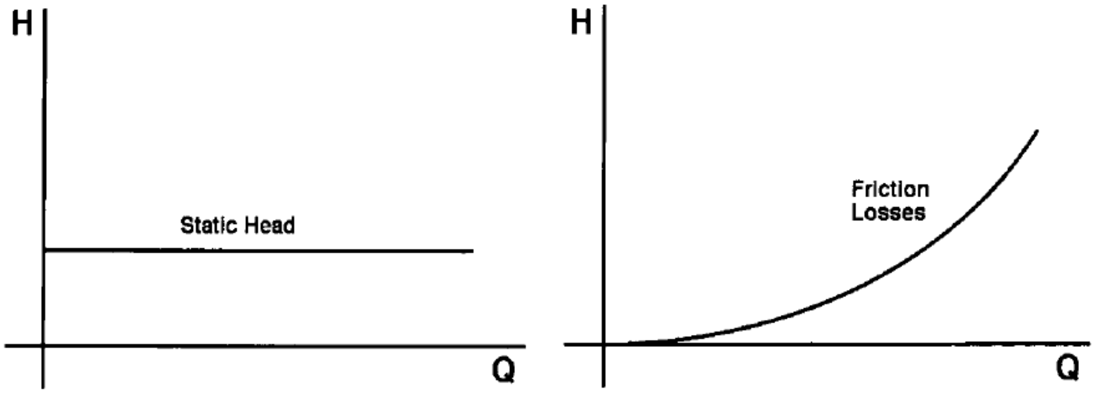

Figure 2.2: Plot of static and friction loss (Mackay, 2004).

To determine the energy saving potential associated with a pumping system the hydraulic system requires modelling given by equation 2-1.

$$H_{process} = H_{static} + H_{friction} \tag{2-1}$$

(Ahonen, Pöyhönen, Siimesjärvi and Tolvanen, 2018)

Where:

$H_{process}$ is the system hydraulic pressure

H_{static} is the system head pressure

$H_{friction}$ is the system friction pressure

The system friction loss consists of the summation of associated piping, valves and equipment losses and is a function of flow rate. Piping losses are governed by pipe length and pipe diameter and the Hazen Williams formula is commonly utilised to express friction in full flowing pipework (Shammas and Wang, 2016). Equation 2-2 defines the Hazen Williams formula to calculate friction head loss in full flowing pipes.

$$H_{friction} = 10.67 \left(\frac{Q}{C}\right)^{1.85} \cdot \frac{L}{D^{4.87}} \tag{2-2}$$

(Shammas and Wang, 2016)

Where:

$H_{friction}$ is the system friction pressure in meters head.

C is the Hazen Williams coefficient of 150 for GRE pipe

L is the pipe length in meters

D is the pipe diameter in meters

Q is the flow rate in m/s

Large butterfly valves are a device most commonly used to control process flow in high pressure and velocity applications. These valves will typically operate at low pressure drops between 30% and 70% opening. (Song, Wang and Park, 2009). A butterfly valve typically consists of a metal disc connected to a shaft that rotates 90 degrees around it axis. As the valve rotates from the fully closed position or 0 degrees to the 90 degrees fully open position the pressure drop across the valve decreases and flow rate through the valve is increased (Pawar, Suryawanshi, Shinde and Vade, 2015). This relationship between pressure drop and flow is known as the flow coefficient and is expressed below in equation 2-3.

$$C_v = \frac{Q}{\sqrt{\Delta P \cdot SG}} \tag{2-3}$$

(Song, Wang and Park, 2009).

Where:

C_v is the valve coefficient.

Q is the flow rate in meters cubed per hour

P is the pressure drop in bars across the valve.

SG is the specific gravity of the fluid.

The flow coefficient of a butterfly valve changes for different valve opening positions and it follows that the pressure across the valve will also change for the same flow rate. Table 2.1 illustrates how the CV changes in 10% opening increments for various different valve sizes.

Size		Cv Value at different degrees of opening								
inch	mm	10°	20°	30°	40°	50°	60°	70°	80°	90°
2	50	0.1	5	12	24	45	64	90	125	135
2 1/2	65	0.2	8	20	37	65	98	144	204	220
3	80	0.3	12	22	39	70	116	183	275	302
4	100	0.5	17	36	78	139	230	364	546	600
5	125	0.8	29	61	133	237	392	620	930	1022
6	150	2	45	95	205	366	605	958	1437	1579
8	200	3	89	188	408	727	1202	1903	2854	3136
10	250	4	151	320	694	1237	2047	3240	4859	5340
12	300	5	234	495	1072	1911	3162	5005	7507	8250
14	350	6	338	715	1549	2761	4568	7230	10844	11917
16	400	8	464	983	2130	3797	6282	9942	14913	16388
18	450	11	615	1302	2822	5028	8320	13168	19752	21705
20	500	14	791	1674	3628	6465	10698	16931	25396	27908
22	550	17	965	2042	4426	7887	13052	20655	30983	34048
24	600	22	1222	2587	5605	9989	16528	26157	39236	43116
26	650	26	1434	3036	6578	11723	19397	29263	46047	50600
28	700	30	1663	3522	7630	12599	20036	30482	46899	58696
30	750	35	1912	4050	8142	13152	20411	31226	47562	63328
32	800	45	2387	4791	8736	13788	20613	31395	48117	68250
34	850	51	2697	5414	9872	15580	23293	35476	54372	77123
36	900	60	3021	6063	11055	17449	26086	39731	60895	86375
40	1000	84	4183	8395	15307	24159	36166	55084	84425	119750
42	1050	350	4095	9040	17108	27150	43640	70500	106890	117500
48	1200	455	5365	11840	22400	30600	51200	92300	140000	154000

Table 2.1: Valve CV for 10° opening increments of various valve sizes (Rates and Valves, 2021)

When system data is unavailable or approximations are acceptable there are well known system relationships that can be implemented to model system components. Equation 2-4 approximates the relationship between friction loss and flow rate and is given below.

$$\left[\frac{Q_2}{Q_1}\right]^2 = \frac{H_{f_2}}{H_{f_1}} \tag{2-4}$$

(Mackay, 2004).

Where:

Q_1 is the initial flow rate.

Q_2 is the new flow rate.

H_{f1} is the initial friction loss

H_{f2} is the new friction loss

The majority of industrial systems includes a combination of static and friction head losses and when this is plotted against the system flow rate the system curve is produced. Figure 2.3 illustrates both a system curve with high friction head and system curve with high static head. The ratio between static and friction head influences the potential benefits that can be achieved with the implementation of variable speed drives (Institute, 2004).

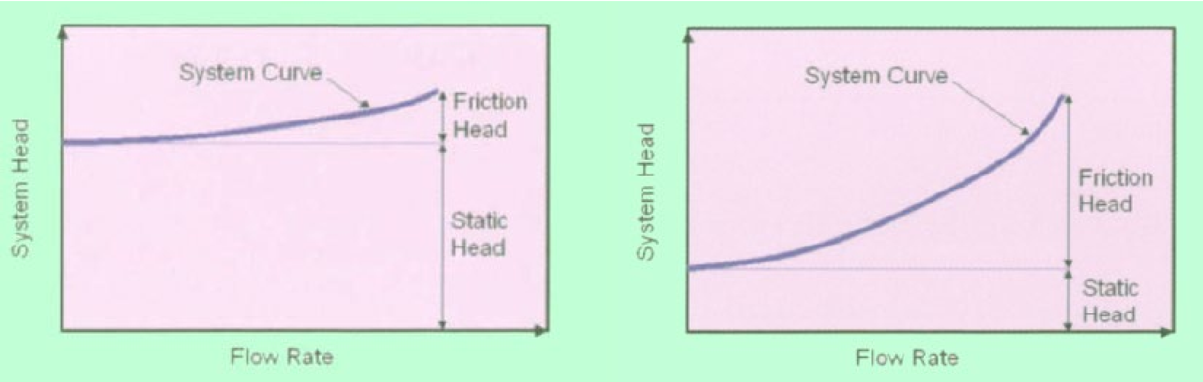

Figure 2.3: High friction and static head system curves (Institute, 2004)

There are two main category types for pumps which are considered either positive displacement or rotodynamic pumps (Institute, 2004). Yara Pilbara Fertiliser SCW pumps are of the rotodynamic centrifugal type and will be the focus of this research.

A centrifugal pump moves liquid from one area to another by rotating one or more impellers inside its volute casing (Mackay, 2004). The liquid is passed through the pump via the casing inlet and impeller where its velocity is increased circumferentially before discharging from the casing outlet at a higher pressure or head (Institute, 2004). Figure 2.4 illustrated a typical centrifugal pump single volute casing and impeller.

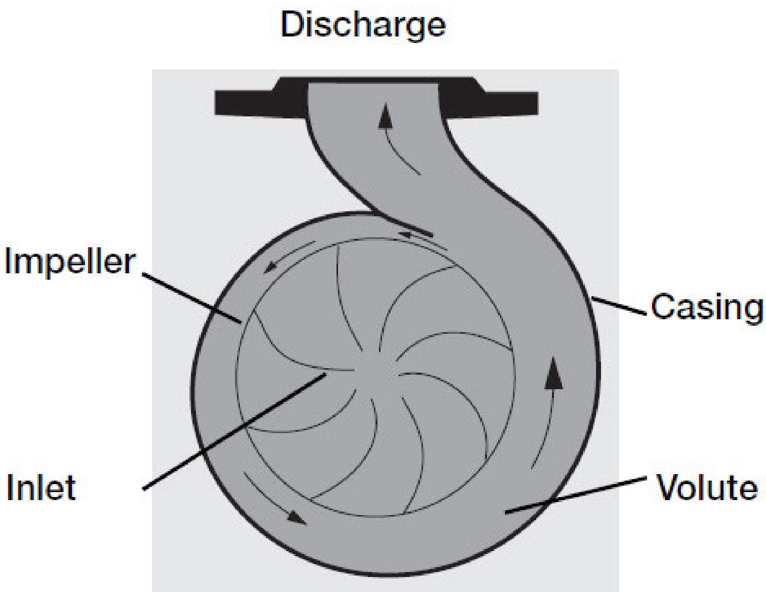

Figure 2.4: Single volute centrifugal pump casing and impeller (ABB, 2006).

There are many designs of centrifugal pumps such as pumps that have various casing and impeller types, and sizes which all impact on the performance of the pump. The typical performance parameters of a pump are head, efficiency, power and the required net positive suction pressure (NPSHR) all of which are a function of flow rate. Figure 2,5 illustrates an example of a typical pump performance curve.

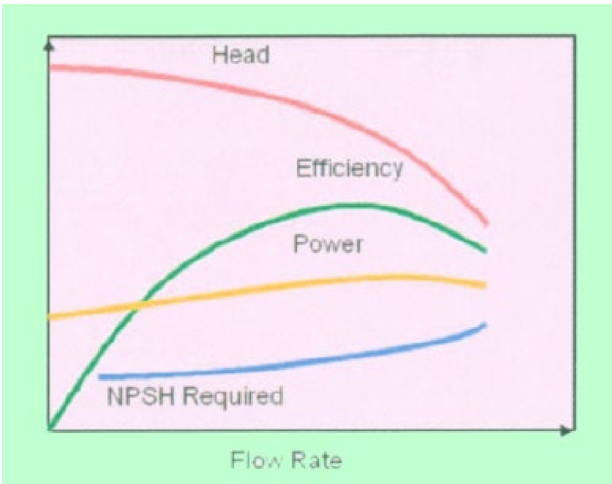

Figure 2.5: Pump performance curves (Institute, 2004)

When a centrifugal pump operates in a hydraulic system the operating point will lie where the pump performance curve intersects with the hydraulic system curve . It therefore follows that the system curve will dictate the performance of the pump which is illustrated in figure 2.6.

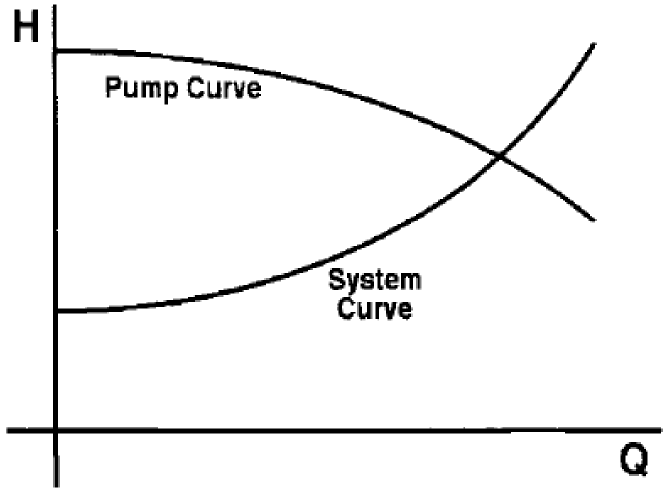

Figure 2.6: Pump and system curve (Mackay, 2004).

As the system or pump curve changes so too will the operation or intersection point. The system curve can be moved by changing the head or friction losses in the system. This can occur for a number of reasons including adjusting control valves, variations in vessel pressures or filter blockages. An increase in friction loss will result in a steeper system curve and hence an increase in system head and decrease in system flow and ultimately wasted energy as is illustrated in figure 2.7.

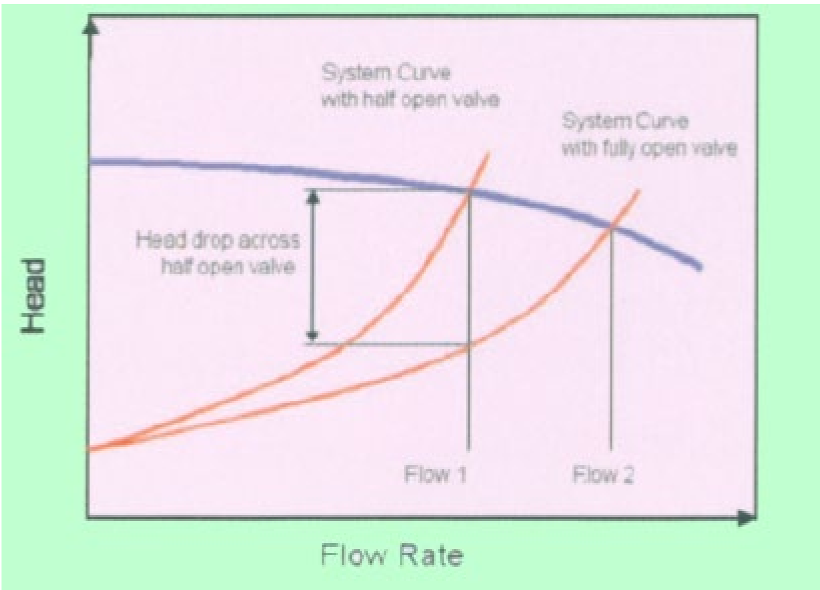

Figure 2.7: Head loss across a throttle valve in a pumping system (Institute, 2004)

A more efficient way to control flow is to reduce pump speed as it has been proven that energy consumption is affected by rotational speed which can lead to large energy savings (Ahonen, Pöyhönen, Siimesjärvi and Tolvanen, 2018). There is a relationship that exists between impeller speed, discharge flow rate, developed head pressure and power consumption and are known as the affinity laws (institute 2004). These are given in the following equations.

$$Q \approx n \tag{2-3}$$

$$H \approx n^2 \tag{2-4}$$

$$P \approx n^3 \tag{2-5}$$

(Institute, 2004)

Where:

Q is the system flow rate

H is the pump head pressure

P is the absorbed power

n is the pump rotational speed

It can be seen that pump flow rate is approximately proportional to speed, head pressure is proportional to the square of pump speed and absorbed power is proportional to the cube of pump speed. It follows that a small change in pump speed will result in a significant reduction in absorbed power in fact a reduction of 20% speed or flow will only require 50% of the power making centrifugal loads a prime candidate for speed control applications (Almeida, 1996). Power consumption can be calculated with equation 2-6.

$$P_Q = \frac{Q \cdot H \cdot g \cdot \rho}{\eta_P \cdot \eta_M \cdot \eta_D} \tag{2-6}$$

(ahemed, 2021)

Where:

P_Q is the absorbed power in Watts

Q is the pump flow rate in m^3/sec

H is the pump head pressure in meters

g is the gravitational constant of 9.81m/s

ρ is the process density

η_P is the pump efficiency

η_M is the motor efficiency

η_D is the VSD efficiency

Assuming the process density, and pump efficiency remain constant, application of the affinity laws in a scenario which requires 70% flow, figure 2.8 illustrates an energy consumption comparison of the four most common control methods concluding that VSD control is the most effective method while throttle control is the least.

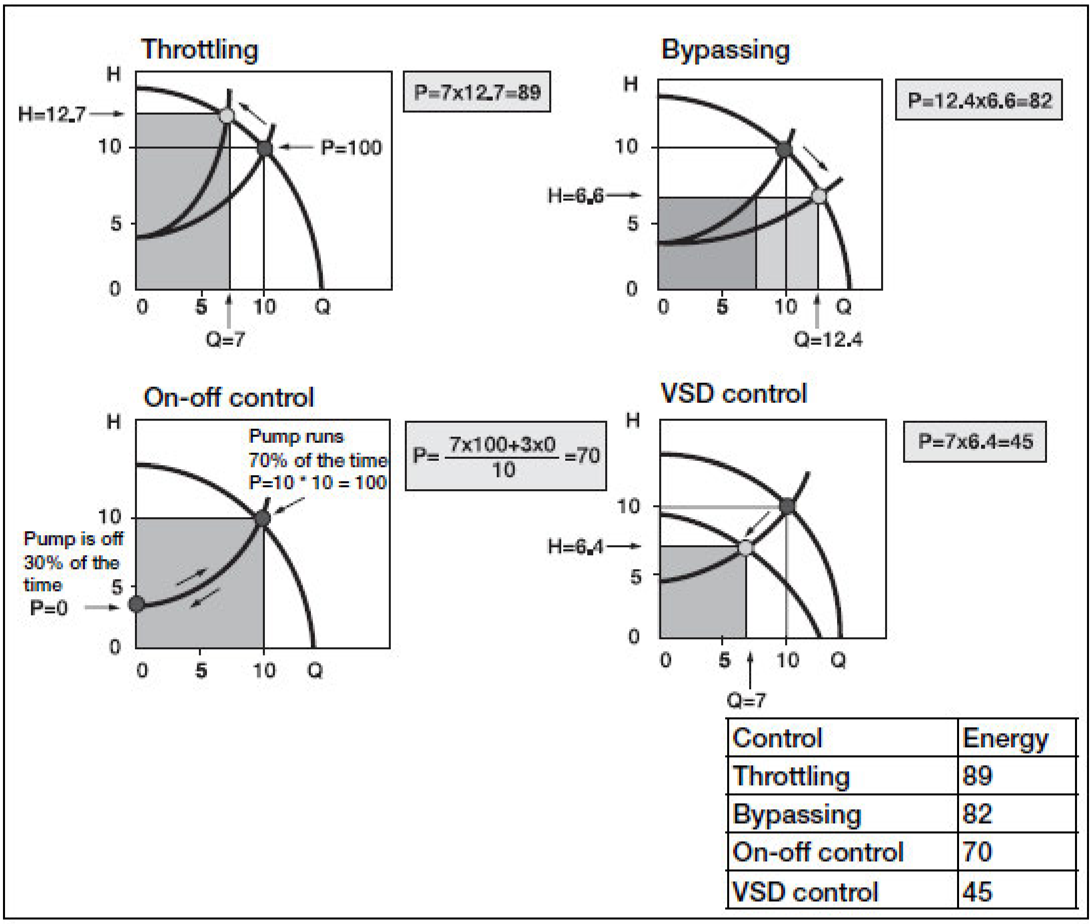

Figure 2.8: Energy consumption comparison of the 4 most common control methods (ABB, 2006).

In practice however pump efficiency, or system flow does not remain constant as you vary pump speed and the Affinity laws can only be used as an approximation. When speed is adjusted above 20% then efficiency considerations are required and a correction required (Ahonen, Pöyhönen, Siimesjärvi and Tolvanen, 2018). Pump Head modelling and efficiency correction for variation in pump speed and flow rates are given in equation 2-7.and 2-8

$$H(Q, n_r) = \left(\frac{n_r}{n_n}\right)^2 \cdot H_{max_n} - \left(\frac{n_r}{n_n}\right)^2 \cdot \left(H_{max_n} - H_{BEP_n}\right) \cdot \left(\frac{\frac{n_n}{n_r} \cdot Q}{Q_{BEP_n}}\right)^2 \tag{2-7}$$

$$\eta(Q, n_r) = 1 - \left[1 - \eta_{BEP_n}\left(\frac{2 \cdot \frac{n_n}{n_r} \cdot Q}{Q_{BEP_n}} - \frac{\left(\frac{n_n}{n_r} \cdot Q\right)^2}{Q^2{}_{BEP_n}}\right)\right] \cdot \left(\frac{n_n}{n_r}\right)^{0.1} \tag{2-8}$$

(Ahonen, Pöyhönen, Siimesjärvi and Tolvanen, 2018)

Where:

n_r is the reduced operating speed

n_n is the nominal operating speed

η_{BEP_n} is the pump efficiency at the best efficiency point at the reduced operating speed

Q is the pump flow rate

Q_{BEPn} is the flow rate at the best efficiency point at the normal operating speed

H is the pump head pressure as a function of speed and flow rate

H_{MAXn} is the maximum pump head pressure at normal operating speed

H_{BEPn} is the pump head pressure at the best efficiency point at the normal operating speed

2.3 Environmental Impact

Fossil fuel electricity production and combustion processes are one of the main industry sources of air pollution and greenhouse emissions and account for approximately 40% of US national carbon dioxide emissions (Zhai and Rubin, 2013). These processes emit carbon monoxide (CO), carbon dioxide (CO_2), sulphur dioxide (SO_2) and nitrogen oxides (NO_x) which are considered primary pollutants as they are dangerous to the health of human beings, detrimental to the environment and can cause undesired effects such as photochemical smog, acid rain, tropospheric ozone and ozone layer depletion (Korpela et al., 2017).

The build-up of greenhouse gases in the atmosphere are universally considered the primary cause of the global warming that has occurred over the past 50 years (Zhai and Rubin, 2013) and action is required to reduce emissions and curb climate change. Climate protection is gaining momentum in other countries with carbon tax being one of the policy measures being discussed (Bachmann, 2020).

It therefore translates that a reduction in energy consumption and steam demand will have a direct reduction of greenhouse gas emissions and a positive environmental impact. It is important to financially quantify the resulting impact to allow its inclusion in the life cycle cost analysis of this proposal. The introduction of price mechanisms to reduce carbon emissions is currently implemented in other countries of the world and is utilised to deter these types of emissions. Table 2.2 illustrates 2020 carbon taxes imposed on European countries.

	Carbon Tax Rate (per ton of CO_2e)		Share of Jurisdiction's Greenhouse Gas Emissions Covered	Year of Implementation
	Euros	US-Dollars		
Denmark (DK)	€23.77	$26.00	40%	1992
Estonia (EE)	€1.83	$2.00	3%	2000
Finland (FI)	€62.18	$68.00	36%	1990
France (FR)	€44.81	$49.00	35%	2014
Iceland (IS)	€27.43	$30.00	29%	2010
Ireland (IE)	€25.60	$28.00	49%	2010
Latvia (LV)	€9.14	$10.00	15%	2004
Liechtenstein (LI)	€90.53	$99.00	26%	2008
Norway (NO)	€48.46	$53.00	62%	1991
Poland (PL)	€0.09	$0.10	4%	1990
Portugal (PT)*	€23.77	$26.00	29%	2015
Slovenia (SI)	€17.37	$19.00	24%	1996
Spain (ES)	€14.63	$16.00	3%	2014
Sweden (SE)	€108.81	$119.00	40%	1991
Switzerland (CH)	€90.53	$99.00	33%	2008
Ukraine (UA)	€0.37	$0.40	71%	2011
United Kingdom (GB)**	€20.12	$22.00	23%	2013
	€35.85	$ 39.21	31%	

Table 2.2: European carbon tax rates as of April 2020 (Carbon Taxes in Europe, 2021).

It can be seen from table 2.2 that the maximum carbon tax is $119 USD per tonne while the minimum is $0.1 USD per tonne and the average is $39.21 USD per tonne.

While Australia does not currently implement a carbon tax scheme these have been successfully implemented in the past and are successfully implemented in other parts of the world. Yara is a global organisation that has other plants that are subject to these types of taxes and it is conceivable that they could be reinstated within Australia in the near future providing a tangible method to quantify environmental benefits.

2.4 Other Life Cycle Considerations

The life cycle cost (LCC) associated with a piece of equipment is the summation of life time costs to purchase, operate, install, maintain and dispose of that particular piece of equipment (Pump life cycle costs, 2001) and is expressed in Equation 2.9.

$$LCC = [C_{ic} + C_{in} + C_e + C_0 + C_m + C_s + C_d + C_{env}] \qquad (2\text{-}9)$$

(Institute, 2004)

Where:

LCC is the life cycle costs

C_{ic} is the Purchasing cost

C_{in} is the installation and commissioning costs

C_e is the energy costs

C_0 is the operating costs

C_m is the maintenance costs

C_s is the loss of production costs

C_d is the disposal costs

C_{env} is the environmental costs

There are also financial factors to consider when preforming the life cycle cost analysis such as current and future energy prices, inflation and interest rates which will impact the results (Pump life cycle costs, 2001). Since these factors are currently unknown and wont be for this project, net present values will be utilised for the purpose of life cycle cost analysis.

The financial feasibility of installing variable speed drives can be measured with the life cycle cost analysis however companies typically evaluate energy savings through key performance indicators such as the payback period. This has the most important contribution toward project feasibility and can be calculated from equation 2-10 below (Nel, Arndt, Vosloo and Mathews, 2019).

.

$$PBP = \frac{C_{TE}}{C_{TS}} \tag{2-10}$$

(Nel, Arndt, Vosloo and Mathews, 2019)

Where:

PBP is the payback period

C_{TE} is the total project expenditure

C_{TS} is the total cost saving

Motor technology is the largest and most important load within industry and the application of variable speed drives poses the most attractive benefit potential to achieve energy savings (deAlmeida, Ferreira and Both, 2005). The use of VSD not only results in energy savings but can also lead to other benefits such as better process control, less wear in mechanical components, a reduction in acoustical noise and improved power factor. Unfortunately VSD's can also introduce some disadvantages such as electromagnetic interference generation, current and voltage harmonics into the supply and the potential reduction of motor efficiency and life expectancy (deAlmeida, Ferreira and Both, 2005). These other effects of VSD implementation can also influence the life cycle costs and require consideration.

Hydraulic forces applied to the pump impeller transferring from the pressure profile within the casing also reduce with speed. These forces are supported by the pump bearings and it follows that a reduction in speed will also increase the bearings life. The bearing life for a rotodynamic pump can be approximated as the bearing life is proportional to the seventh power of speed and is given in equation 2.10 (Institute, 2004)

$$B \approx n^7 \tag{2-11}$$

(Institute, 2004)

Where:

B is the bearing life

n is the pump speed

In addition to this there is a reduction in pump vibration and noise increasing pump seal life given operation remains within tolerable operating limits (Institute, 2004).

The advancement of power electronics switching devices has greatly improved the performance of high speed switching inverter technology. Inverter gate bipolar transistors (IGBTs) can achieve switching frequencies of 2 to 20kHz and are utilised in motor applications over 200kW (von Jouanne, Enjeti and Gray, 1996).

Unfortunately in many retrofit applications inverters are located in a remote location to that of the motor with long cable lengths connecting the two. Due to the combination of high frequency switching and the distributed nature of these cables they act as transmission lines and can result in an increased voltage at the motor terminals having an adverse effect on motor insulation and promote motor bearing deterioration (von Jouanne, Enjeti and Gray, 1996).

The governing factors that determine whether high motor terminal voltages will occur are the cable length, the cable parameters, the motor resistance and the inverter pulse rise time. In general if the time it takes for the inverter pulse to travel down the cable is greater than 3 times the inverter pulse rise time then a full reflection will occur and the pulse amplitude will double (von Jouanne, Enjeti and Gray, 1996). Inverters implementing insulated gate bipolar transistor technology (IGBT's) have rise times of less than 0.1 micro seconds (Persson, 1992).

The following equations can be used to calculate the cable parameters and the critical inverter pulse rise time that ensures voltage increase is minimal.

$$\Gamma_L = \frac{R_L - Z_o}{R_L + Z_o} \tag{2-12}$$

(von Jouanne, Enjeti and Gray, 1996).

Where:

Γ_L is the load reflection coefficient

R_L is the load resistance

Z_o is the cable characteristic impedance given by equation (2-13)

$$Z_o = \sqrt{\frac{L_C}{C_C}} \tag{2-13}$$

(von Jouanne, Enjeti and Gray, 1996).

Where:

L_C is the cable inductance per meter

C_C is the cable capacitance per meter

Now the critical rise time can be calculated in equation (2-14).

$$t_r = \frac{3 \cdot l_c \cdot \Gamma_L}{v \cdot 0.2} \tag{2-14}$$

(von Jouanne, Enjeti and Gray, 1996).

Where:

t_r is the inverter pulse critical rise time

l_c is the cable length in feet

Γ_L is the load reflection coefficient

v is the inverter pulse velocity given by equation (2-15)

$$v = \frac{1}{\sqrt{L_C \cdot C_C}} \tag{2-15}$$

(von Jouanne, Enjeti and Gray, 1996).

The determination of increased motor terminal voltage due to installation of variable speed drive will decide if the installation of filters are required to reduce the transmission line effect and the associated costs will be considered.

Speed reduction of a self cooled motor will proportionally decrease the rotational speed of its cooling fan and has the potential to increase its operating temperature resulting in a reduction of the operational lifetime and efficiency of the motor. The insulation level determines the allowable temperature rise of a motor (Kriel, 2021) and is given below in table 2.3.

Insulation class	E	B	F	H
Ambient temperature, T_a	40°C	40°C	40°C	40°C
Admissible peak temperature, DT	75°C	80°C	105°C	125°C
Safety margin (hottest winding point)	5°C	10°C	10°C	15°C
Maximum admissible temperature, T_m	120°C	130°C	155°C	180°C

Table 2.3: Motor insulation class (Kriel, 2021).

Figure 2.9 illustrates the equivalent circuit of an induction motor and demonstrates that there are two components that comprise motor losses. Namely the variable I^2R copper losses and fixed hysteresis and eddy current iron losses when the supply voltage and frequency are held constant. These losses dissipate heat through the motor casing and are cooled by a motors cooling system.

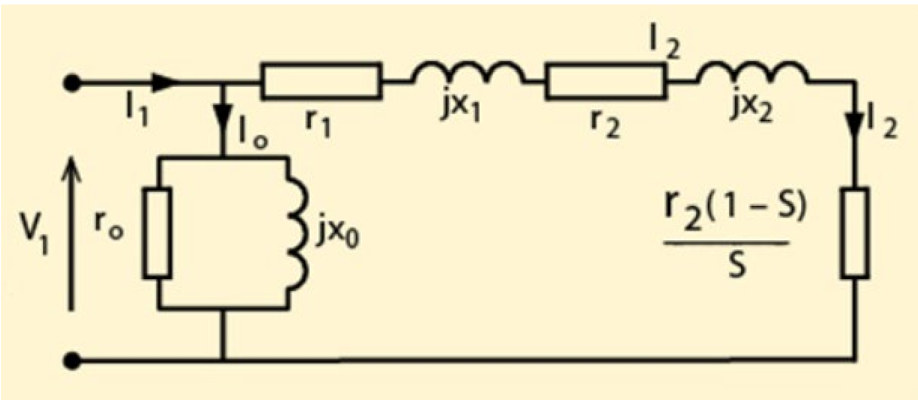

Figure 2.9: Equivalent induction motor circuit model (Bowtell and Ramakrishnan, 2017)

Affinity law equation 2-3 shows that the fan flow rate is directly proportional to fan speed and it follows that cooling capacity reduces accordingly. On the contrary Affinity Law equation

2-5 shows a cubic relationship between power consumption and motor speed and hence a reduction in motor speed will also reduce the load and I^2R heat dissipation losses.

As you can see from figure 3.2, iron losses are a function of voltage and frequency and are a function of the voltage and hertz ratio controlled by the VSD, while the copper losses are a function of load current which will reduce as speed is decreased. Therefore a reduction in motor speed will have minimal effect on motor cooling (Kriel, 2021) and this is reinforced in Appendix D motor operating manual voltage and frequency table that states a 5 % decrease in frequency will only result in a slight temperature rise.

The introduction of system harmonics can have adverse side effects on equipment connected to the system. These include excessive heating, pulsating and reduced torque in motors and generators, voltage stress in capacitors and malfunction of electronics, switchgear and relays (Blooming and Carnovale, 2021).

Total harmonic distortion is a source of system pollution that is represented as percentage of the voltage magnitude at the fundamental frequency and is given below in equation (2-16).

$$THD\% = \frac{\sqrt{\sum_{n=2}^{\infty} V_n^2}}{V_1} \qquad (2\text{-}16)$$

(ABB, 2021).

Where:

THD% is the total harmonic distortion percentage

V_n is the voltage magnitude of the nth order harmonic.

V_1 is the voltage magnitude of the fundamental harmonic.

The strength of an electrical system determines the risk of voltage instability and it follows that a weak system is prone to voltage instability (Saha and Yan, 2021). System strength can be evaluated by comparing the ratio between the system fault current and the output power from the variable speed drive and is given below in equation 2-17.

$$SCR = \frac{SCMVA}{MW_{NST}} \qquad (2\text{-}17)$$

(Blooming and Carnovale, 2021).

Where:

SCR is the short circuit ratio

$SCMVA$ is the short circuit MVA rating

MW_{NST} is the VSD output rating in MW

A high SCR will ensure the risks associated with harmonic distortion are minimised and that the total harmonic distortion is kept below IEEE 519-2014 acceptable limits of 5% for medium voltage systems (Blooming and Carnovale, 2021). IEEE 519-2014 guidelines also show that a system with SCR less than 20 has a 5% current total harmonic distortion level limit.

2.5 Summary

The installation of variable speed drives in this application has the potential to significantly reduce the total associated costs of the system. However there are several factors that require consideration to analyse the feasibility of this proposal and a complete life cycle analysis will be required.

The literature review conducted focused on the key factors that contribute to the life cycle cost of the proposal including energy consumption, environmental impact, harmonics, motor temperature rise and transmission line effects. The research identified methods to model the hydraulic and pumping systems, calculate energy consumption and quantify environmental and equipment impacts. These methods will form the basis of the analysis and are detailed in section 3 Methodology.

Chapter 3

Methodology

3.1 Introduction

The use of electrical motors in pumping systems consumes a large portion of industry power and potentially provides the opportunity for significant cost savings and other benefits through the implementation of variable speed drives (deAlmeida, Ferreira and Both, 2005). To assess the suitability of variable speed drive implementation in a specific pumping system both the hydraulic and electrical systems require analysis. This chapter details the necessary data collection and system analysis that is required to effectively and critically review this proposal. The expected outcomes of this analysis are then detailed in section 3.4 followed by a summary in section 3.5.

3.2 Data Collection

The analysis of a pumping system and its life cycle costs requires a model representation that can be used to accurately determine the response of the system under operational conditions. In order to model the system, data collection of the associated equipment and process parameters that comprise the system are required. The pumping system simplistically consists of the electrical drives and motors, the centrifugal pumps, the piping system and other equipment and the process fluid to be transferred through this system which all require individual consideration.

The electrical induction motor and proposed variable speed drive are required to drive the centrifugal pump at varying loads and speeds which results in a change of electrical parameters. This can both positively or negatively impact the system and equipment involved and to financially analyse this impact the following data, which can be found in the Appendices is required.

- Electrical motor data sheet (Appendix J)
- Cable Specifications (Appendix I)
- Variable speed drive parameters (Appendix B)
- Installation costs (Appendix M)
- Purchase costs (Appendix P)
- Maintenance costs (Appendix G and H)

The centrifugal pump, process piping, equipment and fluid combines to produce the hydraulic pumping system (Mackay 2004). It is this system that dictates the work required by the pumps, motors and variable speed drives to move the process fluid throughout the system. This is a function of flow rate and the following data sources found in the Appendices are required to model this relationship.

- Centrifugal pump data sheet (Appendix E)
- Heat exchangers data sheet (Appendix N)
- Condenser data sheet (Appendix O)
- Piping isometrics (Appendix L)

The preceding data will allow the accurate modelling of the system during steady state conditions however to validate the models, real data measurement of the existing system is required which is listed below.

- Motor input current
- Motor operated valve position
- Pump discharge pressure

The collection of the above mentioned information will ensure adequate data is obtained to allow the accurate modelling and analysis of the system and equipment interaction in enough detail to calculate the associated life cycle costs and payback period.

3.3 Method of Analysis

The Life cycle analysis is an effective way to compare alternative pumping systems and provide financial justification for a particular solution (Institute 2004). The life cycle cost is the summation of the costs associated with each component of a systems life cycle. These included the costs to purchase, install, maintain, operate and repair the associated equipment (Pump life cycle costs, 2001). The methods of analyse for these life cycle components are detailed in the following paragraphs.

Energy consumption of a centrifugal pumping system is highly dependent on the hydraulic system and the system flow rate and will be the focus of this analysis due to the significant contribution to life cycle costs. The hydraulic system consists of many components that influence the hydraulic losses in the system and include the piping network, control valves, system elevation and system equipment such as condensers and heat exchangers (Mackay, 2004). In order to compare the existing and proposed systems and equipment, analysis and modelling of both the pumping and hydraulic system is required under varying conditions. The model will assist in the development of a system curve throughout the entire flow range and a pump curve for varying speeds . These curves can then be superimposed via Matlab software and the operating point and power consumption determined and compared for both operating configurations. The models and results can then be verified with real data and Matlab Simscape simulations.

The aforementioned system curve components will need to be modelled individually and then summated to obtain a representation of the complete hydraulic system. Due to the limited information available of system equipment at dynamic conditions well proven estimations will be required. In the instance where only equipment single point condition data is provided equation 2-4 will be utilised to obtain the relationship between friction loss and flow rate in the system model, while table 2.1 and equation 2-3 will be implemented to model the system losses introduced from the flow control valves. System piping will be estimated from pipe length and pipe diameter and calculated from equation 2.2. Static loss will be obtained directly from the elevations given in relevant isometric drawings and the fluid density obtained from process data sheets.

System flow rates and pump efficiencies vary at dynamic pump speeds and can be modelled by equation 2.7. The affinity laws in equations 2.3, 2.4 and 2.5 no longer hold true when operating at lower speeds because the pump efficiencies can vary significantly. This efficiency reduction will be accounted for and modelled with equation 2.8 resulting in an accurate pump curve.

Superposition of both curves will allow the operation point to be determined which will provide the system flow rate and pump head pressure. These parameters along with pump efficiency, motor and drive data can then be inserted into equation 2.6 to calculate power consumption and the associated energy consumption per year. This will form the basis for financial comparison between the existing and proposed systems.

Other contributing factors that will also be considered are the purchasing and installation costs of the equipment which will be obtained from vendor advice. Maintenance costs such as pump bearing and seal life from equation 2.10, motor life and efficiency reduction and the costs associated with the potential installation of transmission line filters determined from equation 2.13 which will only be considered if the critical rise time is exceeded. Environmental costs will be determined from the emissions associated with generating power and a reasonable carbon tax applied at a rate equal to the average European CO_2 tax rate given in table 2.2.

The above methods of analysis will ensure an accurate model of the entire system and other contributing factors are obtained for comparison. The models presented will be compared against Matlab Simscape simulations and real plant data where applicable with the expected outcomes detailed in section 3.4.

3.4 Expected Outcomes

The combination of data collection described in section 3.2 and the methods of analysis described in section 3.3 will ensure the necessary data is available to apply the desired analysis and validate the expected outcomes.

The purpose of this dissertation is to determine if upgrading the existing constant speed induction motor driven pumps to adjustable speed driven pumps is financially feasible through the method of life cycle cost and payback period analysis. In literature review it is clear there are significant energy improvements associated with reducing a motors speed in centrifugal pumping applications. However the extent of energy improvements is greatly dependant on the ratio of system friction to head loss as the pump efficiency is poor at reduced speeds in head lossy weighted systems (Institute 2004). In this particular application the system utilises extremely large piping systems with low friction loss and has a transfer elevation head loss of 30 meters which is not conducive to a system that has high energy saving potential. Additionally I anticipate this will give lower environmental benefits and have high initial purchase and installation costs.

Installation of variable speed drives in remote locations can introduce increased motor terminal voltage because of variable speed drive high frequency switching and the inherent nature of long cable lengths acting as transmission lines. The cable lengths in this particular application are very long and it is expected that increased voltages are likely, to the extent that expensive filtering methods will be required.

This can also introduce additional harmonics onto the network which can negatively affect other equipment on the grid causing undesired operation and reduced life expectancy. Due to the strength of the grid I expect this impact to be minimal and not of concern to the feasibility if this proposal.

The literature review aligns with the expected outcomes discussed in this chapter and completion of the data collection and analysis methods will validate these expectations.

3.5 Summary

Comprehensive and accurate data collection will ensure the necessary information is obtained to implement the analysis methods described in section 3.3. On completion of the analysis the expected outcomes will be realised allowing for the performance of a life cycle cost and payback period analysis and conclusion of the financial feasibility proposal.

Chapter 4

Energy Consumption

4.1 Introduction

To accurately determine the energy consumption associated with a pumping system each individual component of the system requires modelling before the interaction of each element can be considered and ultimately the energy consumption determined.

In the following sub chapters the piping and pumping systems parameters are analysed, calculated and modelled utilising manufacturers documentation and proven engineering equations that are detailed in Chapter 2 Literature Review and Matlab software. The models are then validated by comparison with actual plant parameters to confirm their accuracy This will ensure the data is correct prior to determining the associated energy savings of the proposal.

4.2 Hydraulic System Modelling

The sea cooling water system consists of heat exchangers, condensers, cooling towers, control valves and large interconnecting pipe work that transfers flow around the system. This liquid transfer system comprises both elevation and friction head losses that requires overcoming by the pump discharge pressure to allow liquid to flow around the system.

Analysis and modelling of the system losses relative to system flow will allow the relationship with the pumping system to be determined. Each component of the piping system will be analysed separately by computing a series of fluid dynamic equations in Matlab that have been identified in the literature review. The results will then be combined proportionally to the flow distribution to produce the system curve as can be seen in figure 4.1.

To model the friction head loss associated with the system vessels equation 2-4 was implemented which provides an exponential relationship between equipment friction loss and system flow. Equipment datasheets were referenced to obtain the nominal operating differential pressure and corresponding flow rates which were then extrapolated over the entire operational flow rate. Table 4.1 details the necessary parameters extracted from the equipment datasheets.

Equipment Type	Pressure (mH2O)	Flow (m3h)
Captive Power Plant Condensers	7.8	4726
Fresh Cooling Water Exchanger	10	1612
127MC Condenser	7.2	13335.25
103MJCC Condenser	7	0.05
103MJTC Condenser	7	13335.2

Table 4.1: Equipment nominal pressures and flows.

Identifying the motor operated control butterfly valves actual position and associated flow coefficient (Cv) at this position gives the relationship between valve position, pressure drop and flow rate. Since the valves operated at a fixed position table 2.1 was referenced to determine the valves Cv while equation 2.3 gives the pressure and flow relationship. Equation 2.3 was rearranged to give equation 4.1 and model the pressure drop across the valve throughout the entire flow rate.

$$P = \frac{10.12 \cdot Q^2}{{K_v}^2 \cdot SG} \tag{4-1}$$

Where:

K_v is the valve coefficient C_v in metric units.

Q is the flow rate in meters cubed per hour

P is the pressure drop across the valve in bar.

SG is the specific gravity of the fluid.

Table 4.2 details the constants required to determine a 48inch butterfly valve flow and pressure relationship.

Valve Size (inches)	Valve Position (deg)	CV
48	50	30600
48	90 (fully open)	154000

Table 4.2: 48 inch butterfly valve CV at 50 degree valve position.

The valves where modelled at both the 50 degree position and the 90 degree position to allow the associated difference in pressure drop to be determined.

The piping system consists of over 1000 meters of glass reinforced epoxy (GRE) interconnecting pipe work ranging from 6 inches to 72inches in diameter that transfers sea water in parallel and series paths around the system. This piping introduces an additional pressure loss into the system that also requires overcoming by the centrifugal pumps. The piping pressure loss is a result of the friction between the fluid flow and piping wall and is a function of pipe diameter and fluid flow rate and is modelled by the well-known Hazen Williams formula given by equation 2-2. The piping network also consists of many pipe fittings and bends that contribute to the overall friction of the system however, due to the lack of information and onerous task of calculating the component contribution they have been excluded from the system modelling and a 10% safety factor applied to the results.

Additionally there is a pressure loss associated with the elevation of the system between the starting and destination points of sea water transfer known as static head. The static head is constant and in this application is represented by the elevation difference in meters of water between the cooling tower basin and the top of the cooling tower which equates to 30 meters of water.

The total pressure loss of the hydraulic system is a combination of the losses associated with each individual system component and is illustrated in figure 4.1 below.

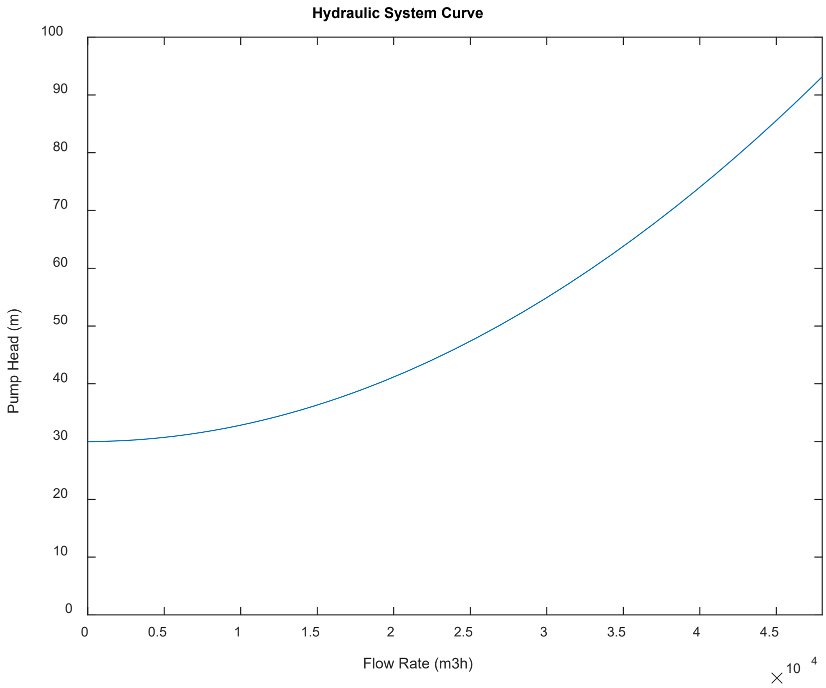

Figure 4.1: Hydraulic System head pressure model produced in Matlab

The functions outlined in this chapter have been utilised to model the complete hydraulic system. This will allow the interaction with the pumping system detailed in chapter 4.2 to be determined.

4.3 Pump Modelling

The pumping system consists of 3 large main centrifugal pumps and 1 smaller emergency centrifugal pump which combined, pump in parallel approximately 30000m^3 per hour of sea water into a common header and around the hydraulic system described in section 4.1. In normal operation the system operates in duty standby configuration with 2 of the large 2.7MW pumps providing duty operation while the third is available on standby. The Emergency pump is only required for site power generation failure scenarios which occurs very infrequently and will not be considered in this dissertation. The pump modelling encompassed the pressure and flow relationship at both nominal speed and reduced speed as well as the reduced pump efficiency associated with this reduction.

The pump curve at nominal speed was obtain from manufacturers data and can be found in Appendix E, however to ascertain the pump and hydraulic system curve relationship this curve required a model replication. To model the pump curve at nominal and reduced speed, equation 2.7 was utilised which calculates the pump head pressure as a function of flow and pump speed utilising the pump parameters illustrated in table 4.3.

Parameter Description	Equation 2.7 Symbol	Value	Units
Max Pump Head at normal pump speed	H_{MAXn}	69.4	Meters water column
Nominal Operating Speed	n_n	594	Revolution per minute
Efficiency at the best operating point at nominal speed	η_{BEP_n}	0.875	percentage
Pump flow rate	Q	0 to 24000	Meters cubed per hour
Pump flow rate at the best efficiency point	Q_{BEPn}	17000	Meters cubed per hour
Head pressure at best efficiency point	H_{BEPn}	47.5	Meters water column

Table 4.3: Manufacturers pump parameters utilised to model the pump

Keeping the pump speed constant at 594 RPM equation 2-7 reduces to equation 4-2 below.

$$H(Q) = H_{max_n} - \left[\left(H_{max_n} - H_{BEP_n} \right) \cdot \left(\frac{Q}{Q_{BEP_n}} \right)^2 \right] \quad (4\text{-}2)$$

Where:

Q is the pump flow rate

Q_{BEPn} is the flow rate at the best efficiency point at the normal operating speed

H is the pump head pressure as a function of speed and flow rate

H_{MAXn} is the maximum pump head pressure at normal operating speed

H_{BEPn} is the pump head pressure at the best efficiency point at the normal operating speed

A Matlab model of each pump utilising equation 4-3 as a function of flow rate is illustrated below in figure 4-2.

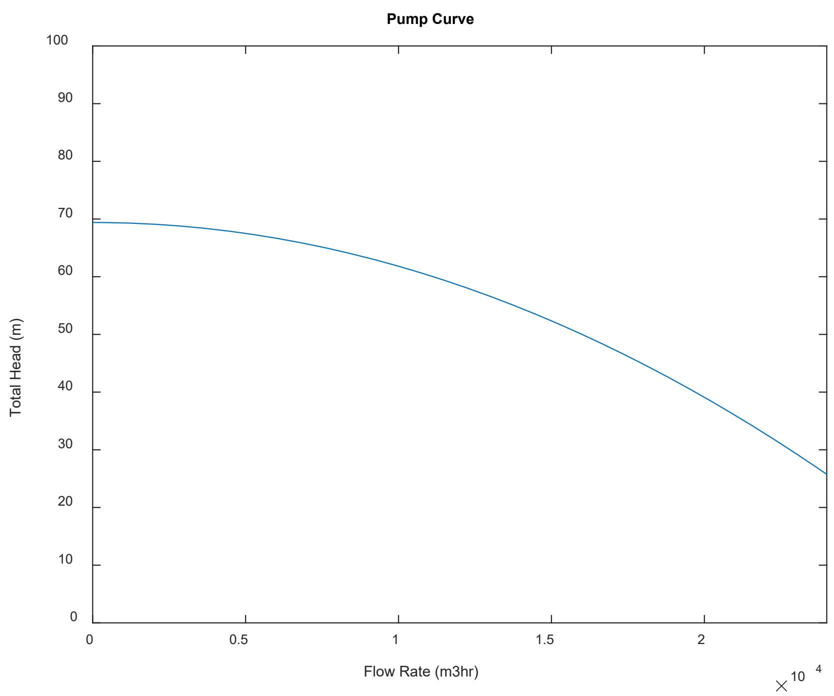

Figure 4.2: Pump head pressure model produced in Matlab

Since the pumps operate in parallel configuration the discharge head will remain constant however the flow rate is the summation of both pumps. Figure 4.3 illustrates the Matlab model of the 2 pumps in parallel operation.

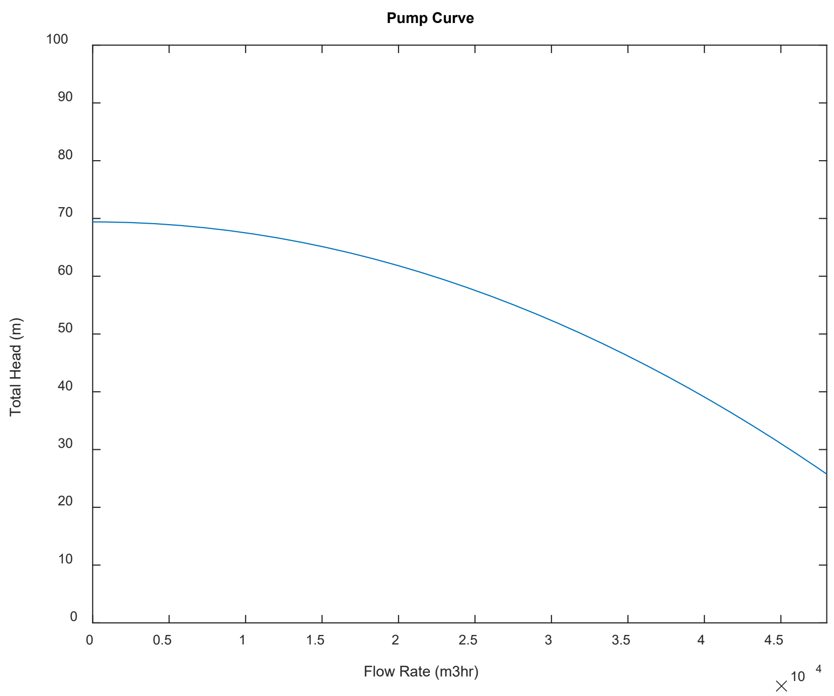

Figure 4.3: Two Pumps in parallel head pressure model produced in Matlab

Modelling the pump at reduced speeds was achieved by firstly implementing the affinity law relationship that head pressure is proportional to the square of pump speed as in equation 2-4. Manipulation of this equation results in equation 4-3 which is used to model the pump head as a function of pump speed.

$$H(n) = H_{max} \cdot \left(\frac{n_r}{n_n}\right)^2 \tag{4-3}$$

Where:

$H(n)$ is pump head pressure at speed n

H_{max} is maximum pump pressure

n_r is the reduced speed.

n_n is the nominal pump speed

Inserting parameters from table 4.3 into equation 4-3 allows the pump head as a function of pump speed at zero flow rate to be modelled in Matlab and is illustrated in figure 4.4 below.

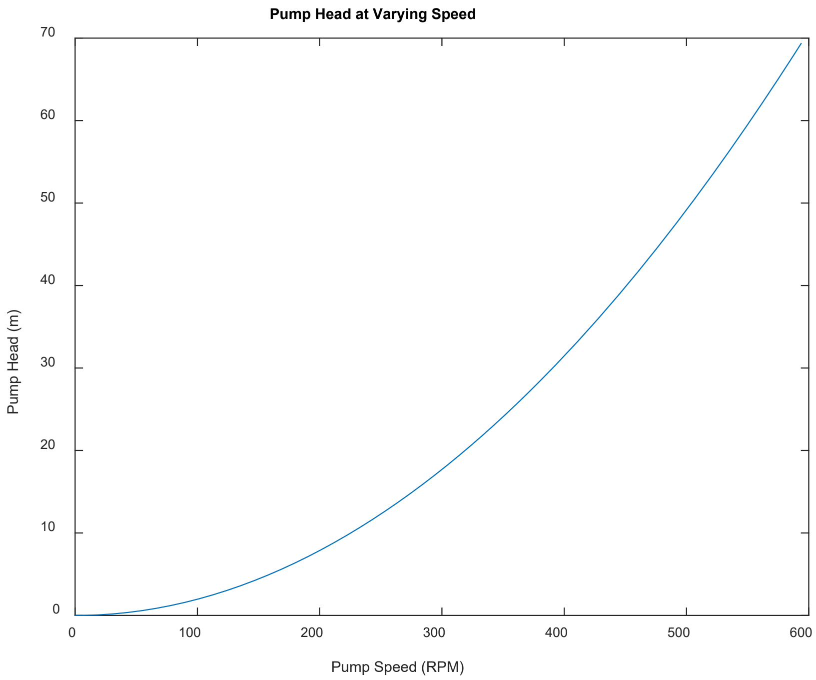

Figure 4.4: Pump head pressure as a function of pump speed model produced in Matlab

When pump speed is reduced so too is pump efficiency. This relationship is expressed by equation 2-8, modelled in Matlab at a desired flow rate of 14183m^3/hr and is illustrated below in figure 4.5.

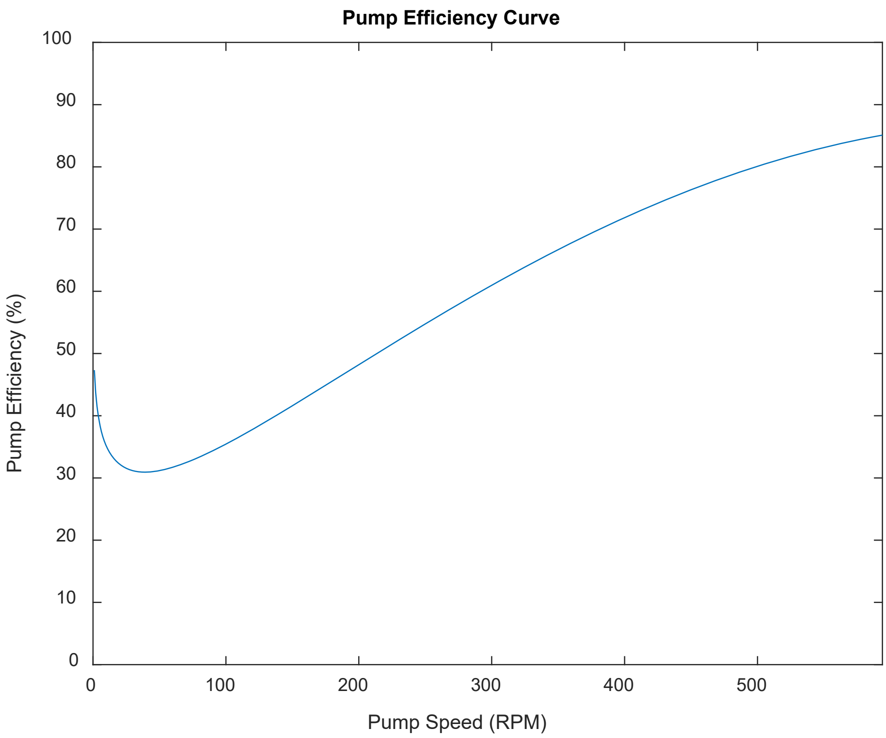

Figure 4.5: Pump efficiency as a function of pump speed model produced in Matlab

Modelling of the pumping system detailed in this chapter along with the hydraulic system in the previous chapter will allow the systems to be overlayed and the system operating point determined. It follows that the associated potential energy savings can then be analysed.

4.4 Energy Savings

The speed reduction of a centrifugal pump will result in a reduction in power consumption with this relationship being described by the affinity law represented in equation 2-5. This law shows that there is a cubic relationship between the two variables and small change in speed will result in a large change in power consumption.

To determine how much pump speed reduction is required to achieve the desired flow rate in the modelled hydraulic system, the modelled pump curve and system curves were overlayed with the intersect being the system operating point as illustrated in figure 4.6.

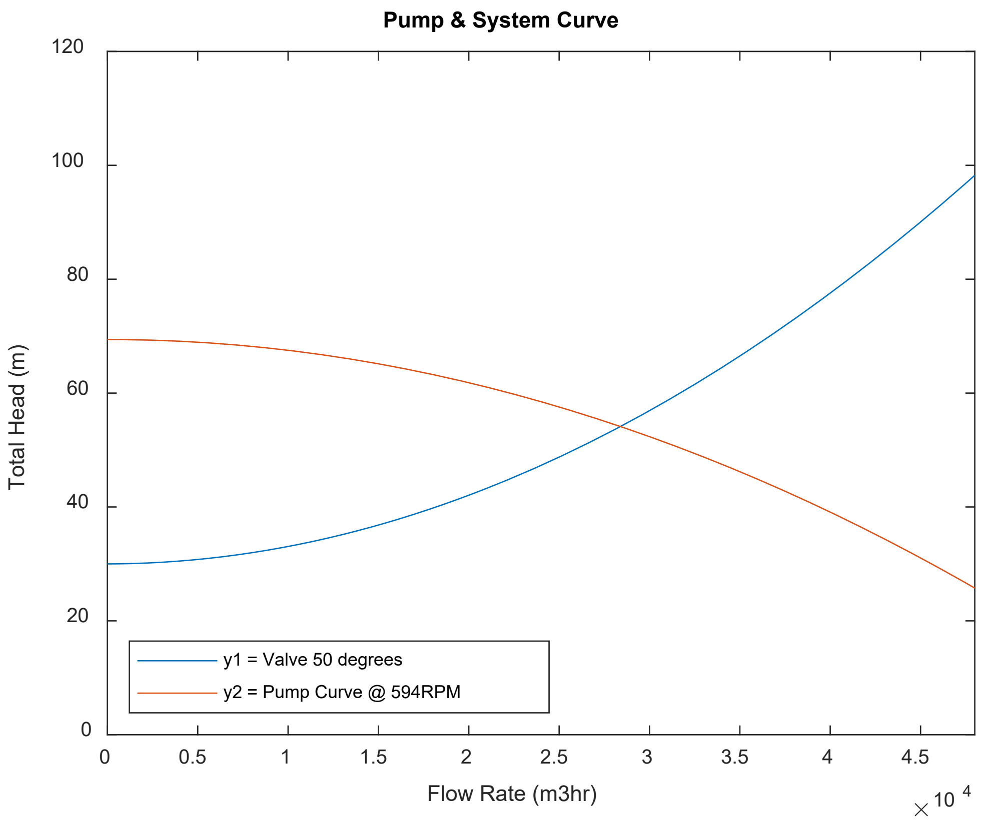

Figure 4.6: Pump and system curves intersecting at the operating point

At this point we can determine the desired system flow rate and transfer that to the hydraulic system curve with the discharge valves fully open and find the new system head . as illustrated in figure 4.7.

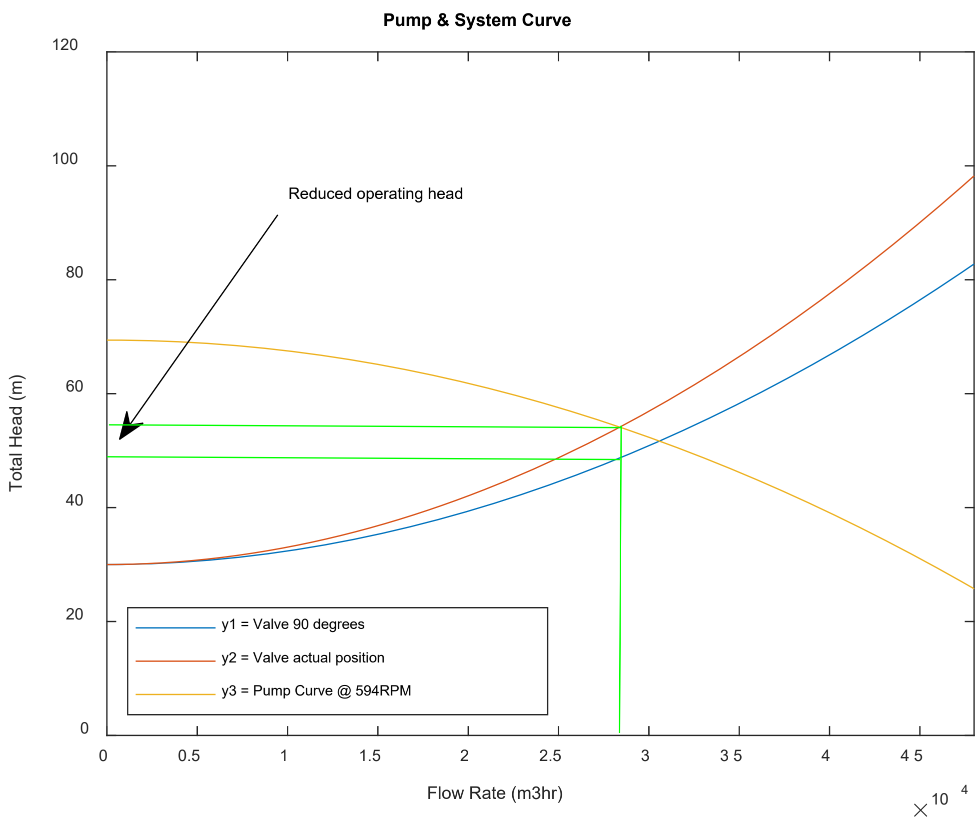

Figure 4.7: Reduced discharge pump head with discharge valves fully open.

At the reduced head the required reduction in speed can be determined from figure 4.4. This gives a required pump speed of 570RPM. Inserting this speed into equation 2.7 and plotting in Matlab gives figure 4.8.

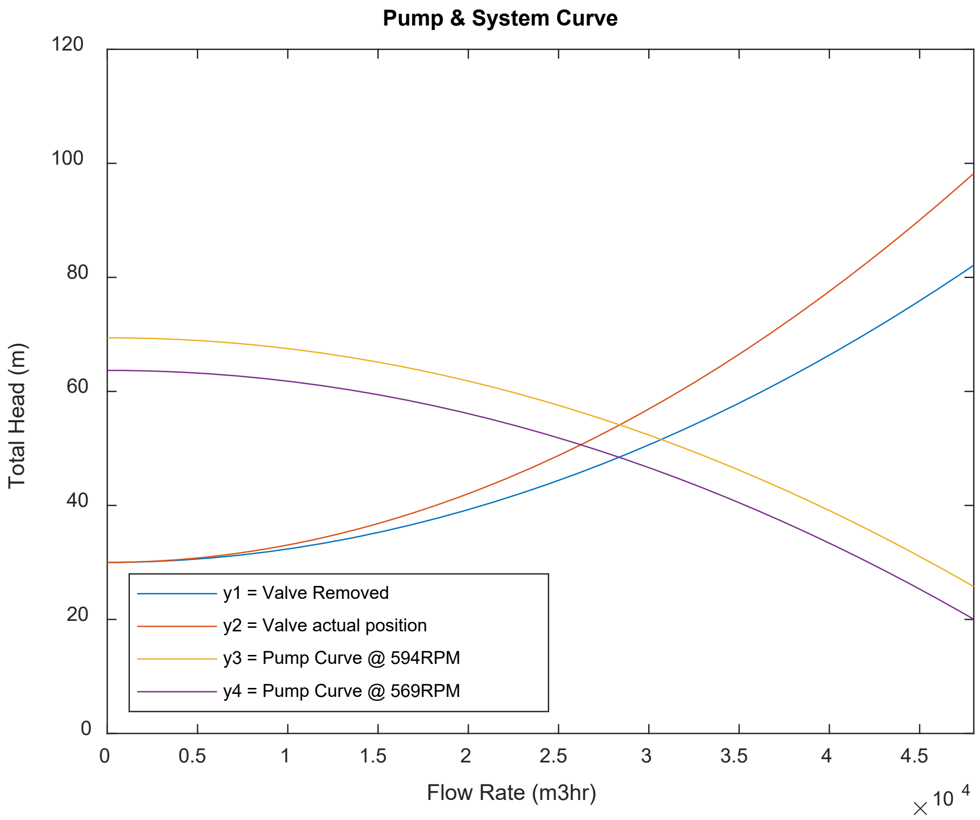

Figure 4.8: Nominal and reduced pump speed overlayed with hydraulic system curves.

Applying the speed reduction of 24 RPM or 4% to the affinity law equation 2-5 gives a power reduction of 11.6 %. However when the pump speed is reduced so to is the pump efficiency which will require consideration. Equation 2-8 expressed pump efficiency as a function of pump speed while equation 2-6 expresses pump power as a function of head pressure, flow rate and equipment efficiency. At 570 RPM the pump efficiency reduces from 87% to 86.2% and evaluating equation 2.6 against both the existing and proposed systems gives the following results tabulated in table 4.4 below.

SYSTEM PARAMETER	EXISTING	PROPOSED1	PROPOSED 2
Valve Position (degrees)	50	90	No Valve
Flow Rate (m3/hr)	14183	14183	14183
Discharge Head (mH2O)	54.1566	48.6810	48.4590
Pump Speed (RPM)	594	570	569

Pump Efficiency (%)	87	84.1	84.0
Motor Efficiency (%)	96	96	96
VSD Efficiency (%)	NA	96.2	96.2
Power Consumption (MW)	5.0122/2.5061	4.85/2.43	4.82/2.41
Energy Saving (%)	4		
Energy Saving Cost(%)	122000/244000		

Table 4.4: Pump energy consumption and associated parameters

4.5 Model Validation

The system and equipment models presented in this chapter have been developed and applied on the theoretical foundations gleaned from the literature review. In order to ensure these models are accurate and can be utilised in the life cycle cost analysis, model validation is necessary. If the models are found to have excessive error then an error factor will be implemented to ensure the conclusions are accurately presented within predefined limits.

The pumping and hydraulic system are completely dependent of each other and validation of one will also validate the other. To achieve this 2 methods have been deployed to validate the models which are described below.

The first validation method implemented is the comparison of real plant data against that of the modelled data. The motor supply current measured in the supplying substation and the discharge motor operated control valve position is compared against that of the power consumption value generated from the modelled data at the equivalent valve positions given in section 4.4 table 4.4. The results are given in table 4.5 below.

Parameter and Equipment	Valve Position (%)	Measured Current (A)	Calculated Power (MW)	Power Factor (PF)
Motor	50	273	2.496	0.8

Model	50	NA	2.506	NA

Table 4.5: Validation method 1 results of system model.

Motor calculated power in table 4.5 is determined from equation 4-4 below.

$$P = I \cdot V \cdot \sqrt{3} \cdot PF \tag{4-4}$$

Where:

P is motor power

I is motor supply current

PF is power factor

The second validation method compares the modelled system flow rate and power consumption with that generated from a Matlab Simscape Fluids simulation which can be found in Appendix Q. The pump data from the manufacturers data sheets in Appendix E was inserted into the simulation software which utilises the affinity equations 2-3, 2-4 and 2-5 to determine the brake power. The modelled values are compared to that generated from Simscape at the modelled flow rate with the results tabulated in table 4.6 below.

Parameter and Validation Type	Flow Rate (m3hr)	Power (MWh)
Simscape	14183	2.209
Model	14183	2.363

Table 4.6: Validation method 2 results. Simscape Fluid's and project model comparison.

Table 4.6 shows a significant error of 0.154 MWh, however the Simscape model does not factor VSD efficiency and reduced pump efficiency from table 4.4. When these parameters are considered the Simscape brake power value increases to 2.37MWh. It is clear from table 4.5 and 4.6 that the error between actual power and modelled power in both validation methods is minimal and it can be concluded that the system pump, efficiency and hydraulic modelling is acceptable for use in further analysis.

Chapter 5

Considerations other than Energy Efficiency

5.1 Introduction

To comprehensively analyse the financial feasibility of this project and conduct a thorough life cycle cost analysis all contributing factors require consideration. These include environmental costs, maintenance and installation costs, thermal analysis, harmonic distortion and transmission line effects. All these factors can either positively or negatively impact the feasibility of this project from a financial, safety, environment and or reliability aspects and require individual consideration.

5.2 Environment

The ammonia production plant has several sources of carbon dioxide emissions that contribute to the total amount of plant emissions and subsequently global warming and environmental pollution. These are a combination of both process and utilities related emissions and their respective contribution quantities have been summarised site below in table 5.1.

Emission Source	Emission Percentage (%)
Electricity Generation	6.9
Steam & Heat Generation	2.05
Ammonia Production	90.9
Miscellaneous Sources	0.2

Table 5.1: Ammonia Plant emission sources.

Table 5.1 highlights that nearly 7% of total plant emissions are attributed to the generation of site electricity.

Site electricity is generated from two 22MW steam turbine generators that generate a total 123,909.65 MWh per year and one 5MW emergency diesel generator that generates 467MWh per year. The required steam is delivered from two gas fired boilers and waste steam from the processing plant. The necessary steam to produce 21,798 MWh of power generation is provided from the processing plant waste steam while the remaining 102111.2MWh is provided from the gas fired boilers.

The boilers consume 1612885.8 GJ of natural gas per year for power generation purposes operating at an efficiency of 15.8 GJ of natural gas per MWh of generated power while the diesel fuel consumed by the emergency diesel generator consumes 4851.6 GJ of energy per year operating at an efficiency 10.4 GJ of diesel fuel per MWh of generated power.

Carbon monoxide (CO), carbon dioxide (CO_2), sulphur dioxide (SO_2) and nitrogen oxides (NO_x) emissions result from the burning of natural gas. The purpose of this analysis will focus on CO2 emissions as they are directly linked to carbon taxes which have a financial impact and can be included in the cost benefit analysis.

Boiler steam generation emits 50.25kg of CO2 per tonne of consumed natural gas while the emergency diesel generator emits 69.9 kg of CO2 per tonne of consumed diesel fuel. It follows that the total and per MWh unit CO2 emissions for both the steam turbine power generators and diesel generators can be determined which are detailed in table 5.2 below.

Equipment and Parameters	Steam Turbine Generator	Diesel Generator
Total Power Generated (MWh)	123909.7	467
Total GJ of Consumed Energy	1612885.8	4581

CO_2 emissions per GJ (kg)	50.25	69.9
Total CO_2 Emissions (Tonnes)	81047.5	320.2
Combined CO_2 Emissions (tonnes)	81165	
CO_2 emitted (Tonne/ MWh)	0.653	

Table 5.2: Power Generation related CO_2 emissions.

Table 5.2 illustrates that in conclusion 0.653 tonnes of CO_2 are emitted for every MWh of power that is generated on site. Utilising the \$39.21 USD carbon tax average cost of CO_2 emissions per tonne from table 2.2 the cost per MWh in AUD can be determined. from equation 5-1 below.

$$C = E \cdot Ec \cdot Er \tag{5-1}$$

Where:

C is CO_2 emissions cost per MWh of power generated

E is CO_2 emissions tonnes per MWh of power generated

Er is USD to AUD exchange rate

Ec is average cost CO_2 emission carbon tax in USD.

Utilising the current USD to AUD exchange rate of \$1.40, Equation 5.2 shows that the cost of carbon tax per MWh of power generated is \$35.84 AUD. The energy savings from table 4.4 combined with the emissions data in table 5.2 and the average carbon tax gives a significant environmental cost saving of \$31395 AUD per year.

5.3 Maintenance and Installation

The installation of variable speed drives to control motor and pump speed in this application has associated maintenance and installation costs that require consideration. The reduction of pump speed typically results in a decrease in pump forces and vibration levels which will increase bearing and mechanical seal life. Additionally the need for the discharge throttle flow control valves are no longer required and these maintenance costs can be reduced or eliminated.

Appendix F provides a list vendor recommended preventative maintenance tasks that should be performed to ensure continuous operation of the pumps. Appendix G illustrates a list of site based preventative maintenance plans that are actually being preformed while Appendix H details all maintenance activities both corrective and preventative and the associated costs that have been performed over the past 6 years.

To determine cost impact, the valve costs have been eliminated while the pump manufacturers recommended maintenance routines have been costed and the frequencies reduced according to the speed and bearing life relationships given in equation 2-10. Table 5.3 itemises the relevant maintenance costs and the potential cost savings.

MAINTENANCE ACTIVITY	DOL COST (AUD/YEAR)	VSD COSTS (AUD/YEAR)
Discharge Valve Maintenance	7000	$0
Pump Bearing Replacements	25000	17500
VSD Maintenance	0	5000
Soft Starter Maintenance	5000	0
Subtotal	37000	22500
Cost Benefit	14500	

Table 5.3: Maintenance Costs per pump

Purchase and installation of the VSD's are a significant cost that will negatively impact the cost benefit analysis. To determine these costs, VSD manufacturer ABB was consulted to provide a budget estimate for the procurement of the drives while a local electrical contracting company was engaged to provide a budget estimate for the installation and commissioning costs. Table 5.4 summarises these costs that cover the following scope of works.

- Conduct risk assessment and obtain HV access and permit to work
- Disconnection, removal and disposal of existing HV soft starter
- Transport VSD into the substation
- Relocation of LV switchboard
- Installation and connection of VSD
- Installation of 50m of 185mm HV cable between VSD and switchgear
- Modification of interconnection control wiring

- Testing and commissioning, with an allowance for ABB commissioning engineer
- Provide testing certificates, notice of completion and site logbook entry
- Provide as built documentation.

EQUIPMENT	COST ($AUD)
VSD	261000
Installation and Commissioning	43500
Total	304500

Table 5.4: Purchasing and installation costs per VSD.

The above maintenance and installation costs detail the associated expenses that are required or can be saved through a reduction in maintenance requirements and supply, installation and commissioning of the equipment. This can now be considered in section 6 life cycle cost analysis to help determine the payback period.

5.4 Transmission Line Effects

The installation of variable speed drives in remote locations that are long distances from the motor can result in increased voltages on the motor terminals. This can lead to insulation breakdown and discharge currents through motor bearings significantly reducing the operational life of the equipment and impacting the life cycle costs. In order to determine if this will occur and if expensive filtering techniques are required, transmission line effects analysis is required.

Section 2 literature review equations 2-12, 2-13, 2-14 and 2-15 show that the inverter critical rise time is a function of cable and load parameters and can be used to determine the critical inverter rise time in which voltage rise due to transmission line effect is likely to occur.

Cable parameters were extracted from equivalent cable data sheets and cable schedules in Appendix I while the load parameters were obtained from the machine parameters in Appendix J. Table 5.5 summarises this data below.

Parameter	Value

Cable Inductance (H/feet)	85.95×10^{-9}
Cable Capacitance (F/feet)	1.58×10^{-10}
Load Resistance (ohms)	2.89
Cable Length (feet)	492.13

Table 5.5: cable and load parameters

The above data can now be implemented to determine the load reflection coefficient, cable characteristic impedance and the critical rise time of the application The results are tabulated below in table 5.6.

Parameter	Value
Load Reflection Coefficient	-0.7796
Cable Characteristic Impedance	23.32
Inverter Pulse Velocity (m/sec)	271.36×10^{6}
Critical Rise Time (sec)	21.2×10^{-6}
Inverter Rise Time	0.1×10^{-6}

Table 5.6: Transmission line effect parameters

Table 5.6 concludes that the IGBT inverter rise time of 0.1 micro seconds will be lower than that of the 21.2 micro seconds critical rise time and a full voltage reflections will occur. This will result in increased generator terminal voltage. and the requirement of the more expensive sine wave filtered option VSD.

5.5 Thermal Analysis

The reduction of a self cooling induction motors speed will reduce the motors overall cooling capacity according to equation 2-3 which shows fan flow rate is directionally proportional to fan speed. This can increase motor temperature rise, reduce motor efficiency, operational life and impact the life cycle cost analysis of this proposal. Section 4.4 Energy Savings concludes that motor speed will be reduced by 24 RPM or 4% which will result in a 4% cooling capacity reduction. To confirm acceptable temperature rise will be maintained, thermal analysis is required.

The motor equivalent circuit illustrated in Figure 3.2 shows that motor losses in the form of heat dissipation are categorized into 2 components. Namely iron and copper loss or no load and load losses respectively. Table 5.7 below illustrates the motor equivalent circuit machine parameters obtained from Appendix J and will provide data input for the thermal analysis.

Machine Parameter	Locked Rotor	Full Speed
R1 (ohms)	0.0526	0.0639
R2 (ohms)	0.0573	0.0697
X1 (ohms)	1.2532	1.5240
X2 (ohms)	1.3379	1.22
Ro (ohms)	8.2330	10.0129
Xo (ohms)	35.5411	42.0192
S (%)	100	1.67
Phase Voltage	3810.5	3810.5

Table 5.7: Sea cooling water induction machine parameters

Analysing the equivalent circuit with the parameters in table 5.7 allows the associated losses at nominal voltage and frequency can be determined. These are tabulated in table 5.8 below.

Loss Type	Power Loss (KW)	Power Loss (%)
Copper Loss	92.440	69.36
Iron Loss	40.829kW	30.64
Total Loss	133.269	100

Table 5.8: Motor losses at nominal voltage and frequency

Reducing motor speed and voltage by a factor of 4% to achieve the required flow rate and maintain constant motor torque capability we can calculate the new full load current from equation 2-5 and 4-4, and the new inductive reactance values which are tabulated below in table 5.9

Machine Parameter	Full Speed
R1 (ohms)	0.0639
R2 (ohms)	0.0697
X1 (ohms)	1.4630

X2 (ohms)	1.1712
Ro (ohms)	10.0129
Xo (ohms)	40.3223
S (%)	1.67
Phase Voltage	3658.08

Table 5.9: Sea cooling water induction machine parameters at 4% reduced speed and voltage.

The corresponding motor full load current and losses can be calculated again to determine if cooling capacity remains sufficient. These results are tabulated below in table 5.10.

Loss Type	Loss Magnitude (KW)	Loss Magnitude (%)
Copper Loss	76.231	70.52
Iron Loss	31.860	29.48
Total Loss	108.09	100

Table 5.10: Motor losses at reduced voltage and frequency.

Tables 5.8 and 5.10 highlight that a 4% reduction in speed and voltage results in a 25KW or 18% reduction in power loss and it can be concluded that no negative impacts from thermal cooling capacity will be introduced and essentially will not be considered In the life costs analysis.

5.6 Harmonics

Increased system harmonics can have adverse side effects to the operation of equipment operating on the network which can result in a reduced operational life cycle. Determination of harmonic levels below acceptable limits will ensure there is no reduction in motor or other equipment's performance.

A strong grid reduces the voltage instability of the system and can be measured from equation 2-17. Inserting relative vendor provided VSD data and system short circuit current into this equation gives system strength which is tabulated below in table 5.11.

VSD OUTPUT POWER (MW)	SHORT CIRCUIT CURRENT(MVA)	SYSTEM STRENGTH
2.85	40	14

Table 5.11: System strength calculated from equation 2-17.

Equipment and system data was also given to the VSD supplier which allowed a harmonic distortion analysis report to be provided and is illustrated below in figure 5.1 and 5.2 with the results tabulated in table 5.12.

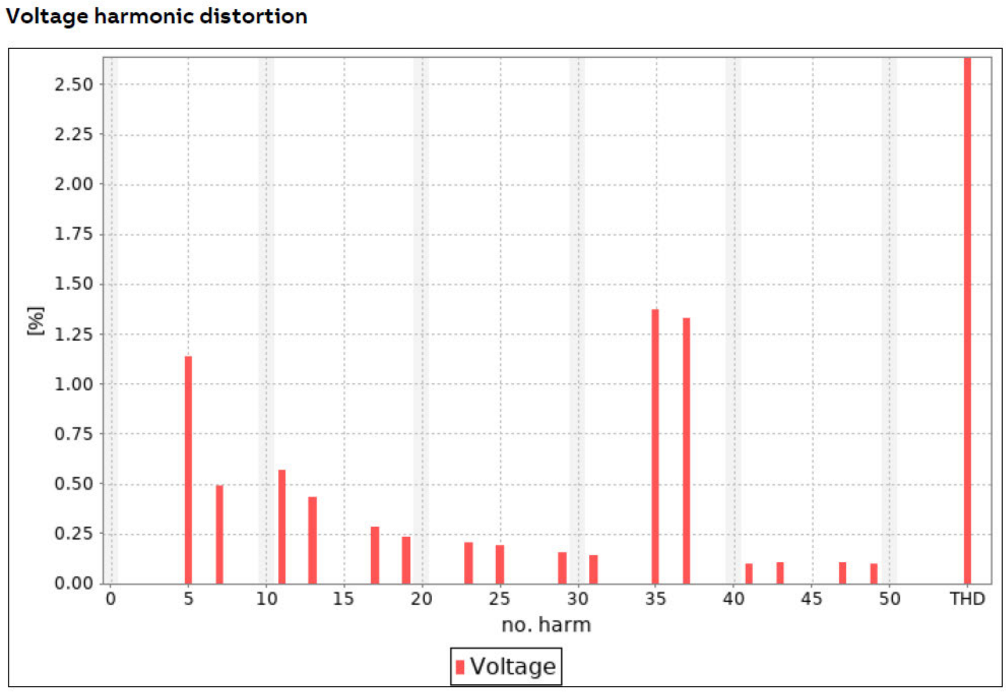

Figure 5.1: System Voltage Harmonic Distortion

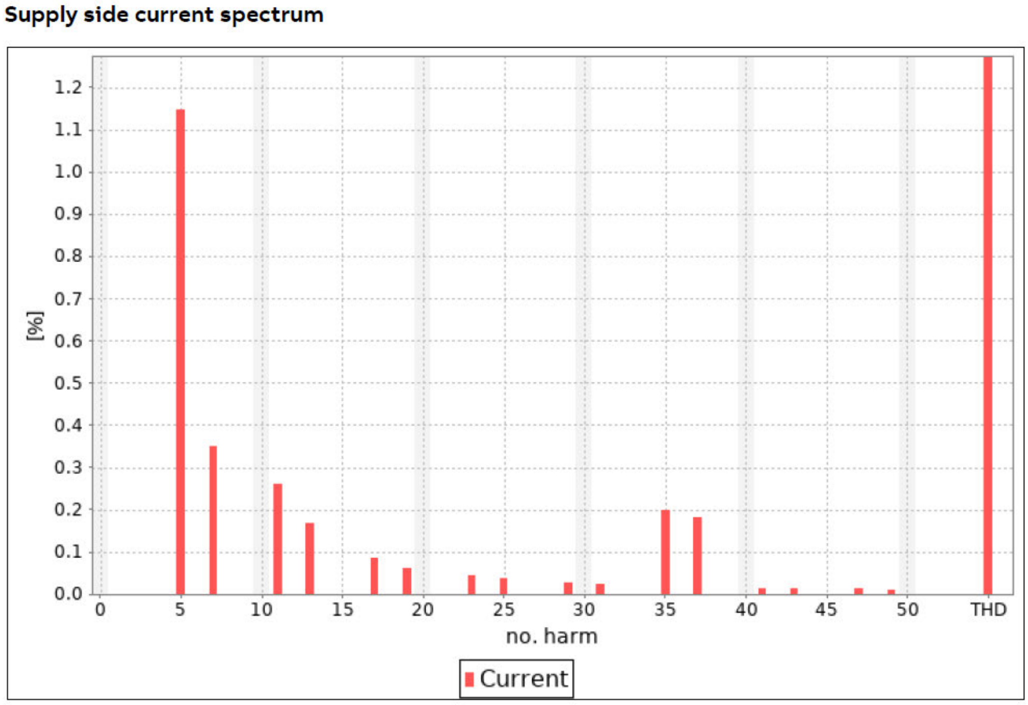

Figure 5.2: System Current Harmonic Distortion.

HARMONIC DISTORTION PARAMETER	VALUE (%)
Voltage	2.64
Current	1.28

Table 5.12: Vendor provided harmonic distortion results

The vendor provided harmonic distortion report shows that total harmonic distortion current and voltage values are low and well within the acceptable limits of 5%. It follows that no equipment operational life reduction factors will be considered in the life cycle cost analysis.

5.6 Summary

In summary the life cycle cost considerations of maintenance, purchasing, installation, environmental, thermal analysis, harmonic distortion and transmission line effects have positive, negative and neutral impact to the proposal.

Maintenance and environmental costs have significant financial benefits as maintenance requirements are reduced and environmental emissions are diminished proportionally to energy consumption savings. Installation and purchasing costs however significantly negatively impact the analysis because there is large initial costs associated with the procurement, installation and commissioning scope of the new VSD as well as removal and disposal of existing equipment. The thermal, harmonics and transmission line effect analysis shows that these aspects will have negligible impact to the proposal as temperature rise will decrease, harmonics levels are acceptable and the inverter pulse rise time is above the critical rise time value.

The analysis presented in this chapter can now be financially quantified to implemented in the Section 6 Life Cycle Costs Analysis

Chapter 6

Life Cycle Cost Analysis

6.1 Introduction

The life cycle costs of a piece of equipment or proposal is the financial summation of all associated aspects and is given by equation 2-9. These include installation, purchase, commissioning, energy, environmental, maintenance and disposal costs which have all been analysed in sections 4 and 5.

In order to perform the life cycle cost analysis these components require per annum financial quantification. This is determined below in sub section 6.2, which will allow an accurate pay back period to be calculated in section 6.3. This can then be presented to management for review and to make an informed decision on the approval of the proposal.

6.2 Costs

In sections 4 and 5 each component of the life cycle cost analysis has been analysed in detail. These included the associated cost impact of energy consumption, environmental emissions, maintenance requirements, purchase, installation, commissioning, harmonics, thermal analysis, and transmission line effects. Each aspect had either a positive, negative or neutral annual contribution to the life cycle costs of the proposal and is extrapolated over the 20 year operational life of the VSD for one pump. This is illustrated below in table 6.1.

LIFE CYCLE COST COMPONENT	ANNUAL COST (AUD)	N YEARS COST APPLIES	TOTAL COST (AUD)
Purchasing	-375000	1	-375000
Installation, Commissioning and Disposal	-43500	1	-43500
Energy Consumption	122000	20	2440000
Environmental Emissions	32000	20	640000
Maintenance	14500	20	290000
Harmonics	0	20	0
Temperature Rise	0	20	0
Total Cost (AUD)	-250000	NA	2951500

Table 6.1: Life Cycle Costs over 20 year period of one pump

Table 6.1 indicates that the life cycle costs of the proposal over the 20 year operational life results in a significant cost saving of 3 million dollars per VSD in service. The pumping system configuration however consists of the three pumps operating in a duty standby configuration. To evaluate the proposal completely this requires consideration and is tabulated below in table 6.2.

LIFE CYCLE COST COMPONENT	TOTAL COST (AUD)
Purchasing 3rd pump	-375000
Installation, Commissioning and Disposal 3rd pump	-43500
Total 20 year Life Cycle Cost (AUD) 2 pumps	5903000
Total 20 year Life Cycle Cost (AUD) 3 pumps	5484500

Table 6.2: Life Cycle Costs over 20 year period for complete application

It can be seen from table 6.2 that the cost savings over the 20 year life cycle of the proposal when all 3 pumps are considered equates to nearly 5.5 million Australian dollars. These costs savings are compelling, however the payback period gives a more measurable approach to quantify the proposal feasibility and is described below in section 6.3.

6.3 Payback Period

The life cycle cost analysis provides a financial measure of the VSD installation proposal over the 20 year operational life of the drive. However companies prefer to evaluate energy saving initiatives by implementation of the payback period method which determines how many years the proposal will take to pay for itself. This technique is proven to give the greatest contribution to the feasibility of a project and is calculated by equation (2-10).

The data from table 6.3 life cycle cost analysis can be implemented into equation (2-10) with the results being tabulated in table 6.3 below.

PAYBACK PERIOD COMPONENT	COST PER YEAR (AUD)
Purchase Cost of 3 VSDs	1125000
Installation and Commission of 3 VSDs	130500
Cost Savings (per annum)	337000
Payback Period (years)	3.7 (years)

Table 6.3: Payback Period in years

The results of equation 2-10 as illustrated in table 6.3 demonstrate that the project proposal gives a payback period of 3.7 years which is longer than the typically preferred industry standard payback period of 12months. This extended payback period can be attributed to the high initial capital purchase and installation expenditure costs which will take 3.7 years to recover.

6.4 Summary

The life cycle cost was analysed over the VSD operational life period of 20 years and was calculated to provide a net present value cost saving of 5.48 million AUD dollars. This is an enticing cost saving over this period, however the payback period gives a direct measure for determining the effectiveness of the proposal. Section 6.3 concludes that a payback period of only 3.7 years is available with this proposal essentially as a result of the expensive initial costs associated with the proposal. Management will need to consider both the extended payback period and the lucrative longer term cost savings to determine if the feasibility of this project.

Chapter 7

Conclusion

7.1 Conclusion

This dissertation demonstrated that there are significant opportunities for cost saving benefits associated with the proposed installation of variable speed drives. These essentially included a reduction in energy consumption, environmental emissions and maintenance costs. Alternatively, the proposal also included high powered equipment that is expensive to install and commission and reduces pump efficiency while introducing additional variable speed drive losses. Implementation of life cycle cost and payback period analysis allowed these factors to be combined to produce a measurable financial indicator of project feasibility

Complete aspects of this proposal were analysed through the methodologies of data collection and system modelling and validation which allowed all elements to be financially quantified or eliminated from consideration. This provided a financial reference for each component which allowed the analysis to be performed. .

Conclusion of the analysis shows that long term financial benefits are very lucrative while, conversely short term rewards are marginal. This is illustrated in section 6 whereby a 5.48 million AU dollar cost benefit is provided over the 20 year operational life of the proposal but has an extended payback period of 3.7 years. It is therefore ultimately the decision of management to consider both the long and short term financial benefits of the proposal and conduct a risk ranking to determine execution priority and acceptance of the project. It is clear however that the installation of variable speed drives in this particular application is financially feasible with several significant benefits available.

7.1 Further Work

The methodology of this proposal focused on the analysis of the installation of variable speed drives onto constant speed pumps to determine the life cycle costs and payback period of the proposal. As this application is operated primarily under steady state conditions there are other methods available to achieve a similar outcome. These include the reduction of pump impeller size or an alternative method to control motor speed such as the installation of a reduced ratio gearbox. These methods could potentially have an improved life cycle cost and payback period than what has been presented here while still providing the operational requirement of the application and should also be considered before a final decision is made.

Additionally there are other applications within our site that operate in a similar inefficient discharge flow throttled constant speed configuration. These include the sea water blowdown, fresh cooling water pumps and demineralised water high voltage pumps that the analysis presented in this dissertation could apply. Following on from this Yara has several ammonia fertiliser, ammonium nitrate and urea plants globally that the results and findings from this dissertation could be applied and amplified

Following from this dissertation, once the proposal approval has been granted then a complete management of change will need to be completed prior to funds being issued. This is a comprehensive risk assessment tool that assesses all aspects of the project and involves all relevant stakeholders to the proposed change

References

ABB, 2006. ABB drives Using variable speed drives (VSDs) in pump applications.

ABB, 2021. Guide to harmonics with AC drives.

ahemed, n., 2021. *The Mathematics of Pumping Water AECOM Design Build Civil, Mechanical Engineering*. [online] Academia.edu. Available at: <https://www.academia.edu/30734272/The_Mathematics_of_Pumping_Water_AECOM_Design_Build_Civil_Mechanical_Engineering> [Accessed 17 April 2021].

Ahonen, T., Pöyhönen, S., Siimesjärvi, J. and Tolvanen, J., 2018. Graphic determination of available energy-saving potential in a reservoir pumping application with variable-speed operation. *Energy Efficiency*, 12(5), pp.1041-1051.

Almeida, A., 1996. *Actions to promote energy efficient electric motors*. [Karlsruhe]: [Fraunhofer-Inst. Systemtechnik u. Innovationsforschung].

Bachmann, T., 2020. Considering environmental costs of greenhouse gas emissions for setting a CO2 tax: A review. *Science of The Total Environment*, 720, p.137524.

Blooming, T. and Carnovale, D., 2021. Application of IEEE STD 519-1992 Harmonic Limits.

Bowtell, L. and Ramakrishnan, R., 2017. *ELE 3803 Electrical Plant Study Book*. 1st ed. Toowoomba: University of Southern Queensland.

deAlmeida, A., Ferreira, F. and Both, D., 2005. Technical and Economical Considerations in the Application of Variable-Speed Drives With Electric Motor Systems. *IEEE Transactions on Industry Applications*, 41(1), pp.188-199.

En.wikipedia.org. 2021. *Ammonia production - Wikipedia*. [online] Available at: <https://en.wikipedia.org/wiki/Ammonia_production> [Accessed 21 August 2021].

Institute, E., 2004. *Variable Speed Pumping*. Burlington: Elsevier.

Korpela, T., Kumpulainen, P., Majanne, Y., Häyrinen, A. and Lautala, P., 2017. Indirect NOx emission monitoring in natural gas fired boilers. *Control Engineering Practice*, 65, pp.11-25.

Kriel, C., 2021. The Influence Of Variable Speed Drives On Electric Motor Operating Temperatures.

Mackay, R., 2004. *The Practical Pumping Handbook*. Science Direct.

Nel, A., Arndt, D., Vosloo, J. and Mathews, M., 2019. Achieving energy efficiency with medium voltage variable speed drives for ventilation-on-demand in South African mines. *Journal of Cleaner Production*, 232, pp.379-390.

Pawar, G., Suryawanshi, P., Shinde, A. and Vade, O., 2015. Performance Parameters of Butterfly Valve - A Review.

Persson, E., 1992. Transient effects in application of PWM inverters to induction motors. *IEEE Transactions on Industry Applications*, 28(5), pp.1095-1101.

Rates, F. and Valves, B., 2021. *Butterfly Valve Flow Rates*. [online] Valvesonline. Available at: <https://www.valvesonline.com.au/references/flow-rates/butterfly-valves/> [Accessed 8 May 2021].

Saha, T. and Yan, R., 2021. System Strength and Weak Grids: Fundamentals, Challenges, and Mitigation Strategies.

Shammas, N. and Wang, L., 2016. *Water Engineering - Hydraulics, Distribution and Treatment*. 1st ed. John Wiley and Sons.

Song, X., Wang, L. and Park, Y., 2009. Fluid and Structural Analysis of a Large Diameter Butterfly Valve. *journal of advanced manufacturing systems*, 08(01), pp.81-88.

Tax Foundation. 2021. *Carbon Taxes in Europe*. [online] Available at: <https://taxfoundation.org/carbon-taxes-in-europe-2020/> [Accessed 19 April 2021].

von Jouanne, A., Enjeti, P. and Gray, W., 1996. Application issues for PWM adjustable speed AC motor drives. *IEEE Industry Applications Magazine*, 2(5), pp.10-18.

Yara Australia. 2021. *Where we operate | Yara Australia*. [online] Available at: <https://www.yara.com.au/about-yara/where-we-operate/> [Accessed 23 September 2021].

Zhai, H. and Rubin, E., 2013. Comparative Performance and Cost Assessments of Coal- and Natural-Gas-Fired Power Plants under a CO2 Emission Performance Standard Regulation. *Energy & Fuels*, 27(8), pp.4290-4301.

2001. *Pump life cycle costs*. [Washington, DC]: Office of Industrial Technologies, Energy Efficiency and Renewable Energy, U.S. Dept. of Energy.

Appendix A

Project Specification

ENG4111/4112 Research Project

Project Specification

For:	Aaron Joseph Chambers
Title:	Feasibility Study to Upgrade HV DOL Driven Pumps to Variable Speed Drives
Major:	Electrical and Electronic Engineering
Supervisors:	Tony Ahfock
Enrollment:	ENG4111 – EXT S1, 2021
	ENG4112 – EXT S2, 2021

Project Aim: To conduct a feasibility to study to install high voltage variable speed drives on existing high voltage asynchronous induction motors driving centrifugal pumps in a throttled flow application.

Programme: Version 1, 17th March 2021

1. Conduct initial background research on relevant pumping systems and contributing factors to life cycle costs associated with both the DOL and VSD pumping applications.
2. Review and model the existing hydraulic system to determine the system requirements, demand and curve.
3. Measure and obtain field data and calculate existing system power consumption and flow output to determine the specific energy of the system.

4. Assess variable speed drive installation and impact to the existing motor and pump in terms of efficiency and operating parameters.
5. Analyze and calculate the specific energy of the proposed VSD system.
6. Review, identify and quantify other associated benefits including maintenance, operation and environmental costs.
7. Conduct a cost benefit analysis of the proposed upgrade and determine the payback period.

If time and resource permit:

8. Consider alternative options to improve the system.
9. Expand the analysis to additional site pumping system applications with similar conditions.

Appendix B

Variable Speed Drive Datasheet

CONVERTER DATA SHEET

1. Converter type

Product	ACS2000
Type code	ACS2000-066-A04B-J4-010
Rectifier type	Diode Front End (DFE) 24 pulse
Supply type	Integrated transformer
Cooling method	Air forced
Design	Industrial standard

2. System

2.1. Output and driven motor 1

Output voltage range	0 … 6'600 V
Output frequency range	0 … 49.7 Hz
Type of motor	Asynchronous
Motor shaft power	2'700 kW
Maximum continuous output current	274 A
Maximum peak output current	305 A (60 s every 600 s)
Motor nominal voltage	6'600 V
Motor nominal speed	590 rpm
Motor nominal frequency	49.7 Hz
Motor power factor	0.89 pu
Motor nominal efficiency	0.97 pu
Operation points	See Appendix for the operation points

Speed encoder interface	None
Motor space heater control and protection	10.0 A, 110 -240V

2.2. Input and supply network

Rectifier type	Diode Front End (DFE) 24 pulse
Supply type	Integrated transformer
Number of input phases	1 x 3
Min supply fault level	200 MVA
Max supply fault level	300 MVA
Supply network voltage	6'600 V
Max cont supply network current	276 A
Voltage tolerance [1]	-10 … +10 %
Supply frequency	50 Hz
Frequency tolerance [1]	-2 … +2 %

[1] According IEC 61800, IEC 60146

STATUS	ID.	DOCUMENT ID.	REV.	LANG.	PAGE
draft	44696-02		A	en	3/11

3. Converter

Converter efficiency	0.962 pu
Surface sound pressure level @1m distance	< 85 dB(A)
Drive system grounding	Hard grounded
Type of motor-side filter	Output sine filter
Winding material of integrated transformer	Manufacturers selection

3.1. VSD enclosure

Type of enclosure	Corrosion protected, 1.5mm thick sheet steel
Cabinet protection class	IP42
Cabinet color	RAL 7035 (light grey)
Painted surfaces	Only front and sides
Door interlocking	Electromechanical door interlocking system
Dimensions main converter (w x d x h)	5'330 x 1'200 x 2'652 mm
Weight main converter	9'842 kg
Weight converter unit Weight transformer unit	3'942 kg 5'900 kg
Type of power cable entry (motor-side)	Aluminum plate undrilled
Location of power cable entry (motor-side)	From bottom
Type of power cable entry (line-side)	Aluminum plate undrilled
Location of power cable entry (line-side)	From bottom
Type of cable entry for auxiliary cables	Aluminum plate undrilled
Location of auxiliary cable entry	From bottom
Location of control cable entry	From bottom

Language of warning labels	English

3.2. Auxiliary and control supply

Auxiliary supply configuration	Single 3-phase
3-phase auxiliary supply voltage	3x 400 V (+/-10%)
Nominal 3-ph auxiliary power	15'000 VA
Peak 3-ph auxiliary power	43'000 VA
Control supply configuration	Single supply (UPS integrated in drive)
Control supply voltage	1x 230 Vac (+/-10%)
Control power	300 VA
Control power ride-through	15 minutes control ride-through (battery based UPS)

3.3. Site conditions

Site altitude	1'000 masl
Min ambient temperature	5 °C

Max ambient temperature	40 °C
Min off-state temperature	5 °C

3.4. Cooling data

Cooling method	Air forced
Losses into air	111 kW
Cooling fan redundancy	No
Cooling air flow	39'000 m3/h

3.5. Control interface

Fieldbus adapter modules	Modbus TCP
Remote connectivity (ABB Ability ™ enabled)	Yes
Control I/O extension	Extension 1
Emergency Off function	Emergency Off (SIL3 / PLe certified)
Emergency Stop function	Emergency Stop (SIL3 / PLe certified)

3.6. Protection functions

Number of controlled MCBs	Control of 1 MCB
MCB requirements: Maximum MCB tripping time Auxiliary switch Status Open indication Auxiliary switch Status Closed indication	 75 ms
Motor temperature supervision	Motor supervision, 8 PT100 inputs
MCB interposing relays	MCB interposing relay + internal trip loop power supply (24V)

3.7. Converter options

Corrosion protected busbars	Corrosion protected
Coated control boards	Yes

Ground ball studs in TEUs	Ball size 25mm

3.8. Certifications

Standards	IEC 61800, IEC 60146
Certification country specific	CE

3.9. Design comments

The auxiliary power for the motor space heater is not included in the datasheet values and has to be considered separately.

Appendix C

Risk Assessment

The hazards associated with this project from a personnel and project perspective have been reviewed and tabulated below in table 4.1. Figure 4.1 illustrates the risk assessment matrix that was referenced to measure the consequence and probability of a hazard or event occurring. The product of the two results in your initial risk rating at which point control measures should be implemented to reduce this as much as reasonably practicable (ALARP) resulting your residual risk rating.

TABLE 4.1 RISK ASSESSMENT			
Initial Risk	Hazard	Control	Residual Risk
20	Substation Access	Complete Induction, obtain escort to access	10
75	Electric shock	Insulated gloves, isolations, test for dead	10
75	Production disturbance	Communicate with operational personnel	10
20	Heat stress	Regular breaks, stay hydrated	10
20	Bad posture and eye strain	Ensure correct ergonomics, take regular breaks.	10
20	Unable to access plant equipment	Early planning and preparation	10
25	Plant shutdown	Make alternative arrangements to access secondary plant	10

75	Loss of job	Make alternative arrangements to access secondary plant	10
75	Loss of data and/or dissertation	Progressive backups of data to cloud based storage	5

Table 4.1: Individual risk assessment.

The ethical considerations associated with this project work are demonstrating integrity and practicing competently.

This project is multidisciplined and involves both electrical and mechanical systems. It is very important to ensure the project research and proposal are presented with factual and well researched information and where models or estimations are made that they are reasonable and validated. This will ensure that management are not making incorrect decisions that could have significant negative financial impact to the business.

In addition, this proposal has the potential to result in large upgrades to existing electrical equipment and infrastructure which will need to comply to Australian electrical standards. This will ensure the installation is installed, tested and commissioned to a high electrical safety standard that will minimise risk to maintenance and operations personnel.

Yara Risk Matrix				Likelihood				
				Less Often	1 yr to 5 yrs	6 months to 1 yr	14 days to 6 months	0 to 14 days
People and Environment			Rating	1	2	3	4	5
				Unlikely	Improbable	Likely	Probable	Frequent
Consequence	Severity 1	• Fatality • Accidental release of hazardous material, liquid or gas to air, water or ground with serious long term environmental impacts.	75	75	150	225	300	375
	Severity 2	• LTI with serious injury consequence resulting in permanent long lasting disability • Release with serious short term environmental impacts.	25	25	50	75	100	125
	Severity 3	• LTI without serious consequence • Release with the potential for short term local impact.	10	10	20	30	40	50
	Severity 4	• Restricted work case (RWC or MTC) • Release with no apparent environmental impact.	5	5	10	15	20	25
	Severity 5	• First Aid Injury (FAI) • Minor release without environmental impact or negative publicity.	1	1	2	3	4	5

75 – 375	Work shall not be started until the risk is reduced and where work is already in progress, the work shall be stopped and urgent action taken to reduce the risk to as low as reasonably practicable.
20 – 50	Efforts must be made to reduce the risk to a level as low as reasonably practicable. This means that a balance of risk vs cost shall be a consideration in the decision making.
1 – 15	Monitoring is required to ensure that the control measures are maintained.

Figure 4.1: Yara risk assessment matrix

Appendix D

Motor Voltage & Frequency Table

TABLE 3. GENERAL EFFECT OF VOLTAGE AND FREQUENCY VARIATION ON INDUCTION MOTOR CHARACTERISTICS

Characteristics	AC Induction Motor			
	Voltage		Frequency	
	110%	90%	105%	95%
Torque, starting and max running:	Increase: 21%	Decrease: 19%	Decrease: 10%	Increase: 11%
Speed: Synchronous Full Load % Slip	 No Change Increase: 1% Decrease: 17%	 No Change Decrease: 1.5% Increase: 23%	 Increase: 5% Increase: 5% Little Change	 Decrease: 5% Decrease: 5% Little Change
Efficiency: Full Load 3/4 Load 1/2 Load	 Increase: 0.5 to 1 point Little Change Decrease: 1 to 2 points	 Decrease: 2 points Little Change Increase: 1 to 2 points	 Slight Increase Slight Increase Slight Increase	 Slight Decrease Slight Decrease Slight Decrease
Power Factor: Full Load 3/4 Load 1/2 Load	 Decrease: 3 points Decrease: 4 points Decrease: 5 to 6 points	 Increase: 1 point Increase: 2 to 3 points Increase: 4 to 5 points	 Slight Increase Slight Increase Slight Increase	 Slight Decrease Slight Decrease Slight Decrease
Current: Starting Full Load	 Increase: 10 to 12% Decrease: 7%	 Decrease: 10 to 12% Increase: 11%	 Decrease: 5 to 6% Slight Decrease	 Increase: 5 to 6% Slight Increase
Temp. Rise:	Decrease: 3 to 4°C	Increase: 6 to 7°C	Slight Decrease	Slight Increase
Max. Overload Capacity:	Increase: 21%	Decrease: 19%	Slight Decrease	Slight Increase
Magnetic Noise:	Slight Increase	Slight Increase	Slight Decrease	Slight Increase

REMARK:
1. The starting and maximum running torque of ac induction motors will vary as the square of the voltage
2. The speed of ac induction motors will vary directly with the frequency.
3. This table shows general effects, which will vary somewhat for specific ratings.

Appendix E

Pump Performance Curve

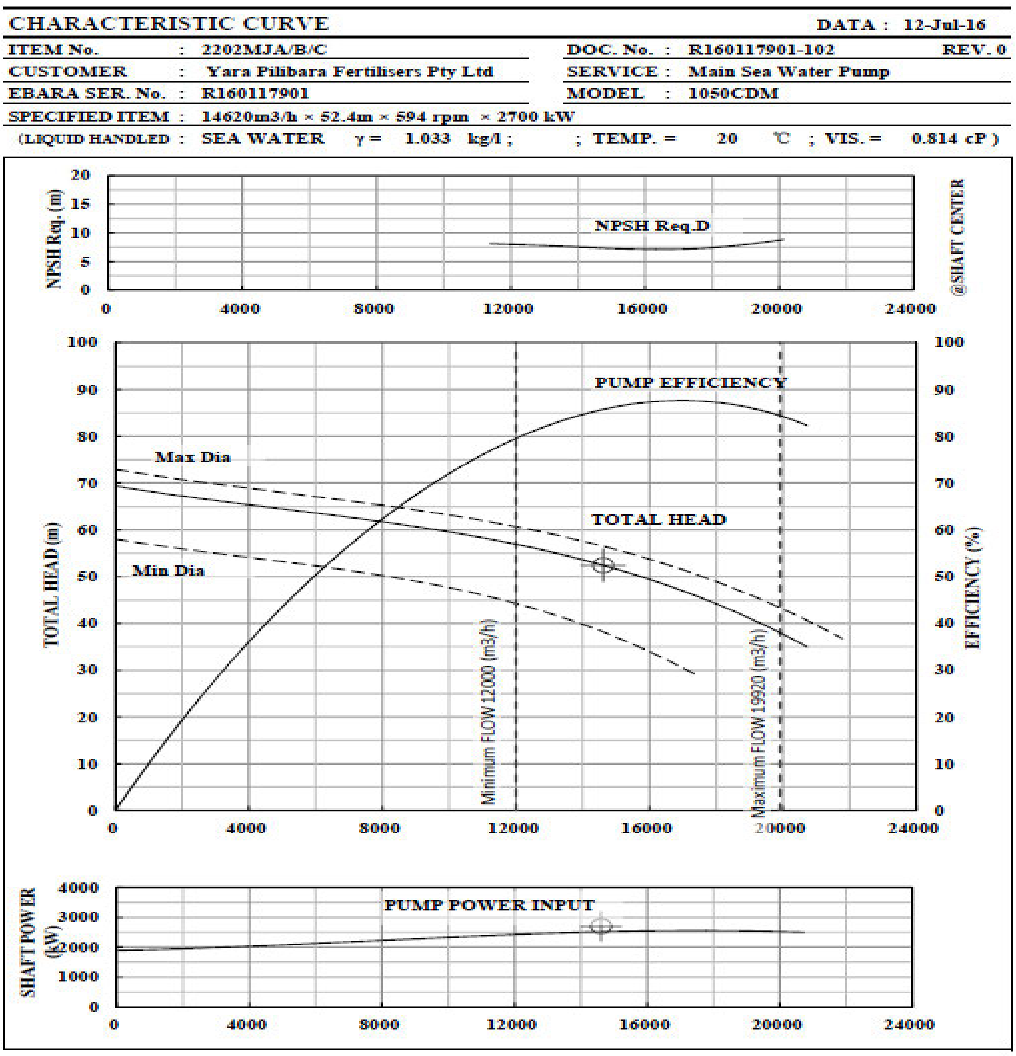

Appendix F

Pump Maintenance Requirements

5. Maintenance

To maintain good pump operation, carry out the following maintenance and checks.

⚠ WARNING

Keep hands, fingers, hair, and tools away from the rotating parts when the pump is operating. Otherwise, serious personal injury may occur.

⚠ WARNING

Cut the power supply so the driver cannot be started by mistake after pump has stopped.

⚠ CAUTION

Drain the pump and piping, as they might crack when internal watar freezes while pump stops in winter.

5.1 Daily Checks

If pressure, current, vibration and noise, etc. are extremely different from normal value, an immediate investigation is required because it is a sign of an impending trouble.

An operation log should be kept for this purpose.

5.1.1 Suction and Discharge Pressures, Current Values

Note

Open the valves for the pressure gauge and compound gauge only when measuring. They can be easily damaged by the dynamic pressure and other causes if they leave open during operation.

Note

When measuring the suction and discharge pressure, it is necessary to remove the remaining air in the small piping between the pressure measurement hole and the gauge. Otherwise, an incorrect pressure value may be measured by the gauge.

(1) Check the values of the suction and discharge pressure gauges, and ammeter values for any swings.

(2) Note especially for the suction side. The movement of the pressure gauge indicator before and behind the strainer should be noted if there is a strainer on the suction side.

5.1.2 Bearing Temperature

Do not worry about the temperature of a bearing housing when the bearing housing can be touched, but measure temperature by installing a thermometer if it can not be touched.

Table 5.1 indicates the surface temperature of a bearing housing with regular general use lubricant.

Table 5.1

Allowable temperature rise (At ambient temperature of not more than 42 ℃)	Allowable maximum temperature
40 ℃	82 ℃

5.1.3 Vibration

Allowable maximum vibration velocity is 9.5mm/s (RMS) on bearing housing. When vibration is large, check for centering of connections, improper piping, loose anchor bolts, etc.

5.1.4 Auxiliary Piping System

Confirm that all valves in the auxiliary piping are properly operating.

Valves used in the small piping system are procured from vendors with strict quality control and used under close check. However, after installation at the site, valve-originated trouble may occur and cause incomplete water sealing to heat the gland. To prevent this, properly adjust the valve opening.

5.2 Periodic Inspections

5.2.1 Replenishment and Replacement of Bearing Lubricant

(1) The oil level should be 7mm above the center of the short level pipe. This can be controlled by setting the oil level adjustment mechanism of the Constant Level Oiler to the lowest position. (Fig. 5.2)
(At shipment, this mechanism is set to the lowest position. Check before supplying oil.)

(2) Remove the glass reservoir and air vent on the top of the bearing housing and fill with oil to the bottom level of the surge chamber. As it takes some time for the oil level to settle after filling, check that the level has stabilized and fill again if necessary.

(3) When the oil level reaches the connecting short pipe, pour oil into the bearing casing using the constant level oiler.

(4) Filling the constant level oiler:
- (a) Fill the glass reservoir with lubricating oil.
- (b) Rapidly insert it into the surge chamber.
- (c) If replenishment from the reservoir is not sufficient, replenish oil again according to steps (a) through (b).
- (d) Tighten the set screw.

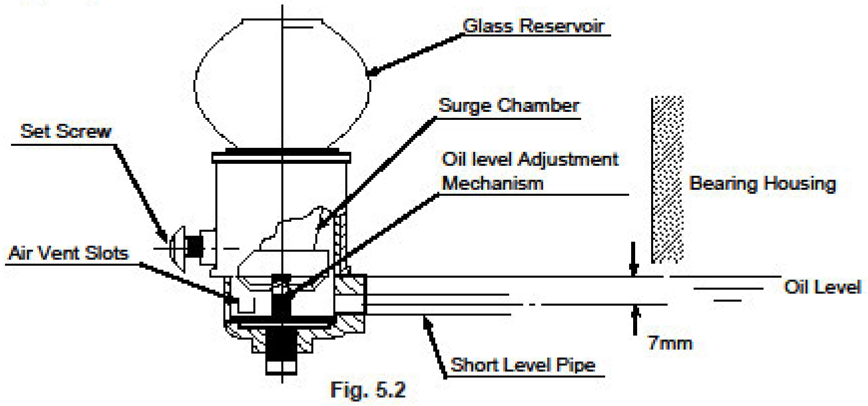

Fig. 5.2

(5) Before driving, the oil level should be 5~8mm above the oil level gauge line.
After the constant level oiler filled, the oil level fill again 5~8mm above the oil level gauge line.

(6) The lubricating oil to be used is JIS K2213 Turbine Oil (ISO VG 46).
The first oil change should be performed after 300 hours of operation, and subsequent oil changes should be carried out every 6 months.
⚠Lubricant maker's bland is as follows.(Refer to LUBRICATION LIST,R160117901-155)
- SHELL : TURBO OIL T46
- MOBIL : DTE OIL MEDIUM
- ESSO : TRESSO 46

Table 5.2

Item No.	Quantity per pump (2 places)
2202MJA/B/C	7000cc

5.2.2 Replacement of Consumable Items

Replace parts, if in the status as shown in Table 5.3.

Table 5.3

Part name	Replacement interval	Approximate replacement interval
Bearing	When abnormal sound occurs or the bearing sounds loud.	Every three years⚠
Gaskets & O-ring	Every overhaul	Every three years⚠
Shaft sleeve & Neckbush	When the surface of the shaft sleeve and neckbush is worn about 3 mm in diameter.	Every three years⚠
Impeller wear ring	When the surface of the impeller wear ring is worn.	Every three years⚠
Case wear ring	When the surface of the case wear ring is worn.	Every three years⚠

These approximate replacement intervals indicate standard periods of time during the pump is operated under normal conditions.

Clearance of wearing parts⚠
Design value : Casing ring 1.60 ~ 1.94mm
Allowable value : Design Value ×2 times.

Diameter of shaft sleeve & neck bush⚠
Design value : Shaft sleeve ϕ260mm(Outer Diameter)
Neck bush ϕ261.8mm(Inner Diameter)
Allowable value : Design Value – 3mm

5.2.3 mechanical Seal

Refer to the instruction manual of the installed mechanical seal. (attached Appendix-A)

5.2.4 Coupling

Refer to the instruction manual of the installed coupling. (attached Appendix-B)

Appendix G

Site Based Maintenance Plans

Description	Functional Loc.	Prior	Bas. start d	Sched. st	Basic fin. d	Total act.co	MaintenanceP
2202MJC - Annual PM of SW cooling pump 3	KTA-F08-M-2202MJC	2	02/09/2019	02/09/2019	08/09/2019	2,896.08	KTAMSC00030
2202MJA - Annual PM of SW cooling pump 1	KTA-F08-M-2202MJA	2	15/10/2019	09/10/2019	20/10/2019	1,210.76	KTAMSC00028
2202MJB - Annual PM of SW cooling pump 2	KTA-F08-M-2202MJB	2	02/12/2019	02/12/2019	08/12/2019	0.00	KTAMSC00029
Annual preventive check of MOV	KTA-F08-E-MOV2401	3	01/07/2018	01/05/2020	02/08/2018	0.00	KTAEISC01300
Annual preventive check of MOV	KTA-F08-E-MOV2402	3	01/07/2018	01/05/2020	02/08/2018	0.00	KTAEISC01301
Annual preventive check of MOV	KTA-F08-E-MOV2403	3	01/07/2018	01/05/2020	02/08/2018	0.00	KTAEISC01302
SD Preventive Maint check of MOV (AUMA)	KTA-F08-E-MOV2402	3	01/01/2018	10/09/2020	30/12/2018	0.00	KTAEISC01739
SD Preventive Maint check of MOV (AUMA)	KTA-F08-E-MOV2403	3	01/01/2018	10/09/2020	30/12/2018	0.00	KTAEISC01740
SD Preventive Maint check of MOV (AUMA)	KTA-F08-E-MOV2401	3	01/01/2018	10/09/2020	30/12/2018	0.00	KTAEISC01740
1Y PM Check MOV2401	KTA-F08-E-MOV2401	2	08/12/2020	15/12/2020	08/12/2020	172.76	KTAEISC01300

Appendix H

Historical Maintenance

Description	Functional Loc.	Prior	Bas. start da	Total act.cos
remove large wooden blocks, supports	KTA-F08-M-2202MJC	2	23/06/2015	0.00
internal coating of 2202 MJA casing	KTA-F08-M-2202MJA	1	10/08/2015	31,614.64
nipple fixing with ceramic base putty	KTA-F08-M-2202MJA	2	11/09/2015	1,022.30
Pump discharge RTRP line failure	KTA-F08-M-2202MJB	1	12/10/2015	899,963.28
SCWpump A remove dischargespool -Inspect	KTA-F08-M-2202MJA	3	12/10/2015	1,355.18
SCWpump C remove dischargespool -Inspect	KTA-F08-M-2202MJC	3	12/10/2015	15,180.46
DE mechanical seal is leaking.	KTA-F08-M-2202MJA	2	24/08/2015	61,078.45
Consumables for2202MJB pipe line rupture	KTA-F08-M-2202MJB	3	12/10/2015	32,372.28
nde bearing need oil topup	KTA-F08-M-2202MJC	2	30/11/2015	135.00
2202mjb NDE gland leak	KTA-F08-M-2202MJB	2	01/12/2015	0.00
Leaking mechanical seal NDE	KTA-F08-M-2202MJB	2	22/02/2016	248,172.60
Overhaul pump as high vib	KTA-F08-M-2202MJC	2	10/12/2015	4,648.19
modi. of 2202MJA/C dis pipe supports	KTA-F08-M-2202MJA	1	10/12/2015	33,422.08
NRV D/S flange is leaking	KTA-F08-M-2202MJB	2	11/04/2016	0.00
NDE bearing oil level very low	KTA-F08-M-2202MJB	1	23/06/2016	0.00
Oil leak from NDE side bearing housing	KTA-F08-M-2202MJB	2	27/07/2016	3,360.97
2202MJA LOW ERRATIC FLOW HI VIBRATIONS	KTA-F08-M-2202MJA	2	05/10/2016	225,905.58
Abnormal Noise	KTA-F08-M-2202MJC	2	20/02/2017	161,810.58
Recond of various spares for SCW Pumps	KTA-F08-M-2202MJA	2	26/04/2016	-8,635.79
Service Contract Corrective	KTA-F08-M-2202MJB	2	05/05/2016	172,467.53
Service Contract Preventive	KTA-F08-M-2202MJB	2	05/05/2016	135,763.22
Low Oil East end	KTA-F08-M-2202MJA	1	23/01/2017	149.50
Low Oil Level 2202mja	KTA-F08-M-2202MJA	2	14/02/2017	149.50
SUCTION VALVE SCW PUMP A	KTA-F08-M-2202MJA	1	18/04/2017	0.00
2202-MJA bearing failure	KTA-F08-M-2202MJA	2	07/08/2017	16,182.33
Repair suction side casing drain.	KTA-F08-M-2202MJA	2	01/05/2017	0.00
To replace SCW pump with compl new pump	KTA-F08-M-2202MJA	2	29/04/2016	1,803,126.12
Check/repair MOV control panel	KTA-F08-E-MOV2402	2	01/06/2017	0.00
2202MJA isolation	KTA-F08-M-2202MJA	2	14/06/2017	0.00
Recondition one set of mechanical seals	KTA-F08-M-2202MJC	2	25/05/2017	4,558.30
Replacement of Main Sea Waetr Pump A	KTA-F08-M-2202MJA	2	29/04/2016	102,610.48
Lifting of the new main sea water pump B	KTA-F08-M-2202MJB	2	24/07/2017	0.00
Lifting of the new main sea water pump C	KTA-F08-M-2202MJC	2	24/07/2017	0.00
To replace SCW pump completely	KTA-F08-M-2202MJB	2	29/04/2016	872,653.48

Replace d/s pressure gauge	KTA-F08-M-2202MJB	2	28/08/2017	0.00
Replacement of Main Sea Waetr Pump B	KTA-F08-M-2202MJB	2	29/04/2016	92,414.88
Noisy coupling	KTA-F08-M-2202MJB	1	16/10/2017	1,745.12
To replace SCW pump completely	KTA-F08-M-2202MJC	2	29/04/2016	870,581.74
2016-PIU-21-Fasteners Sea Water Pumps	KTA-F08-M-2202MJA	2	29/04/2016	13,352.23
Supply - Spool for Main Sea Waetr Pump A	KTA-F08-M-2202MJA	2	29/04/2016	42,096.19
Supply - Spool for Main Sea Waetr Pump B	KTA-F08-M-2202MJB	2	29/04/2016	41,835.23
Supply - Spool for Main Sea Waetr Pump C	KTA-F08-M-2202MJC	2	29/04/2016	41,835.23
Fastners for Main Sea Water Pumps	KTA-F08-M-2202MJA	2	29/04/2016	3,336.06
Refurbish 5 x Bearings SCW Pump	KTA-F08-M-2202MJA	2	03/07/2017	0.00
Sea Water Pump - Vendor Engineer Visit	KTA-F08-M-2202MJA	2	30/05/2017	21,123.45
Check High vibration of SCW pump B	KTA-F08-M-2202MJB	2	19/03/2018	80,677.95
SCW Pump B top priming vent failure	KTA-F08-M-2202MJB	1	12/02/2018	39.74
2202MJB LUBE OIL LEVEL	KTA-F08-M-2202MJB	2	26/02/2018	0.00
Replacement of Main Sea Waetr Pump C	KTA-F08-M-2202MJC	2	29/04/2016	123,959.53
Pump vibration trending high	KTA-F08-M-2202MJB	2	20/01/2019	2,427.11
Replace gear box and valve	KTA-F08-E-MOV2403	3	01/12/2018	0.00
Procurement of Coupling's Transmission	KTA-F08-M-2202MJA	2	22/01/2018	73,512.67
2202MJC - Inspected leak, either seal fo	KTA-F08-M-2202MJC	2	02/09/2019	3,154.89
Check High vibration of SCW pump A	KTA-F08-M-2202MJA	2	22/03/2018	41,512.80
2202MJA LUBE OIL LEVEL	KTA-F08-M-2202MJA	2	02/03/2018	46.87
High vibration in Pump	KTA-F08-M-2202MJB	2	13/06/2019	0.00
Unseize Oiler	KTA-F08-M-2202MJA	2	24/07/2019	265.74
2202MJA - Check change oil	KTA-F08-M-2202MJA	2	05/08/2019	633.02
Load test Motor/pump as required	KTA-F08-M-2202MJC	2	30/09/2019	0.00
SCW "B" Thermostat tripped	KTA-F08-E-MOV2402	1	16/10/2019	126.70
valve installed in reverse direction	KTA-F08-E-MOV2402	3	18/11/2019	23,189.94
NDE OIL LEAK FROM SIGHT GLASS	KTA-F08-M-2202MJC	1	27/04/2020	68.26
Check SCW Pumps for debrish from tower	KTA-F08-M-2202MJA	3	18/11/2019	0.00
Pump have cavitation	KTA-F08-M-2202MJC	2	17/08/2020	0.00
Vibration is trending upward	KTA-F08-M-2202MJA	2	17/08/2020	0.00
SD Preventive Maint check of MOV (AUMA)	KTA-F08-E-MOV2401	3	01/01/2018	0.00
steel rio bar to be removed 5S	KTA-F08-M-2202MJB	2	22/06/2020	135.93

Appendix I

Cable Specifications

Copper 6.35/11kV

Physical & Electrical Characteristics

Product Code	3CCUX11HDA								
Nominal Conductor Area mm²	25	35	50	70	95	120	150	185	240
Nominal Conductor Diameter mm	6,1	7,0	8,2	9,8	11,5	12,9	14,3	16,1	18,2
Nominal Insulation Thickness mm	3.4	3.4	3.4	3.4	3.4	3.4	3.4	3.4	3.4
Approx Cable Diameter mm	51,3	53,7	56,3	60,4	64,4	67,9	71,3	76,7	82,1
Approx Mass kg/100m	430	495	560	675	795	890	995	1220	1440
Max Pulling Tension On Conductors kN	5,3	7,4	11	15	20	25	25	25	25
Max Pulling Tension On Stocking Grip kN	5,3	7,4	11	13	15	16	18	21	24
Max Pulling Tension On Amour Wires kN	11	12	13	15	17	19	21	24	25
Min Bending Radius*: During Installation mm	920	970	1010	1090	1160	1220	1280	1380	1480
Min Bending Radius*: Set In Position mm	620	640	680	720	770	810	860	920	980
Max Conductor Resistance, dc @ 20°C Ohm/km	0,727	0,524	0,387	0,268	0,193	0,153	0,124	0,0991	0,0754
Conductor Resistance, ac @ 90°C & 50 Hz Ohm/km	0,927	0,668	0,494	0,342	0,247	0,196	0,159	0,128	0,0984
Inductance mH/km	0.415	0.397	0.379	0.350	0.333	0.319	0.310	0.300	0.290
Inductive Reactance, @ 50Hz Ohm/km	0.130	0.125	0.119	0.110	0.105	0.100	0.0973	0.0942	0.0910
Zero Seq. Impedance @ 20°C & 50 Hz Ohm/km	3,07+ j0.0836	2,16+ j0,0781	1,56+ j0,0726	1,11+ j0,0635	1,03+ j0.0585	0,995+ j0.0543	0,966+ j0.0515	0,941+ j0.0485	0,917+ j0.0454
Capacitance, Phase To Earth µF/km	0,212	0,231	0,255	0,290	0,325	0,354	0,383	0,419	0,465

RUN NO.	FROM	TO	POWER CABLE (mm^2)						
			6.6KV XLPE (Cu)						
				3x70	3x300				
10302	6.6KV Bd. (SWG-103) in CT S/S	2204-MJAM (400KW)		140					
10302c1	6.6KV Bd. (SWG-103) in CT S/S	LCS							
10302c2	6.6KV Bd. (SWG-103) in CT S/S	I/O RACK-3							
10302sh	6.6KV Bd. (SWG-103) in CT S/S	SPACE HEATER							
10303	6.6KV Bd. (SWG-103) in CT S/S	2201-MJAM (625KW)		240					
10303c1	6.6KV Bd. (SWG-103) in CT S/S	LCS							
10303c2	6.6KV Bd. (SWG-103) in CT S/S	I/O RACK-3							
10303sh	6.6KV Bd. (SWG-103) in CT S/S	SPACE HEATER							
10304	6.6KV Bd. (SWG-103) in CT S/S	SOFT STARTER			15				
10304A	SOFT STARTER	2202-MJAM (2700KW)			150				

Appendix J

Machine Parameters

3 PHASE INDUCTION MOTOR EQUIVALENT CIRCUIT

JOB NO	B7185	FILE NAME	Equivalent_Circuit.doc
DATE	June 24,2009	DESIGN BY	Sean Lin
		CHECKED BY	Jeff Chin

OUTPUT	2700 kW	POLE	10	SYNC SPEED (min-1)	600
VOLTS	6600	FREQ (HZ)	50	TYPE	TIK-FCKNW

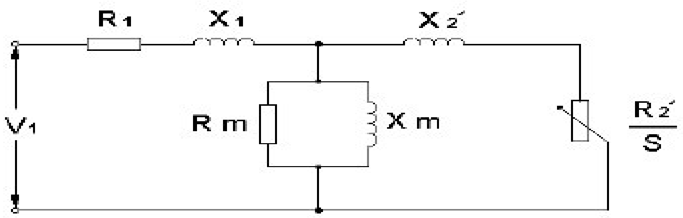

V_1 = 3810.5 Volts

Machine Parameters	Units	At Locked Rotor	At Full Speed
R_1	Ohm / Phase	0.0526	0.0639
X_1	Ohm / Phase	1.2532	1.5240
X m	Ohm / Phase	34.5411	42.0192
R m	Ohm / Phase	8.2330	10.0129
$X_2{}'$	Ohm / Phase	1.3379	1.2200
$R_2{}'$	Ohm / Phase	0.0573	0.0697
S	Per Unit	1	0.0167
Transient Reactance	Ohm / Phase	2.1734	
Sub-Transient Reactance	Ohm / Phase	1.2077	

Appendix K

Matlab Code

```
%%%%%%%%%%%%%%%%%% Dissertation Calculations
%%%%%%%%%%%%%%%%%%%%%%%%%%%%%%%%%%%%%%%%%
clear;
% Butterfly Valve Friction Calculations
CV50 = 30600;  % Valve CV at 50 degrees
KV50 = 0.865*CV50;  % Valve KV at 50 degrees
CV60 = 37000;  % Valve CV at 60 degrees
KV60 = 0.865*CV60;  % Valve KV at 50 degrees
CV30 = 11840;  % Valve CV at 30 degrees
KV30 = 0.865*CV30;  % Valve KV at 30 degrees
CV40 = 22400;  % Valve CV at 40 degrees
KV40 = 0.865*CV40;  % Valve KV at 40 degrees
CV90 = 154000; % Valve CV at 90 degrees
KV90 = 0.865*CV90; % Valve KV at 90 degrees
Q = 0:48000;   % Flow rate vector in meters cube
Q1 = 0:2:48000;
%QQ = 7558; % Pump desired flow rate.
QQ = 14183; % Pump desired flow rate.
QP = QQ;
H1 = 54.1566;
H2 = 48.4589;
g = 9.81;
n = 594; % pump full speed
nn = 0:594; % pump speed
nr = 569; % Reduced pump speed
nnr = 1:594;
sv = zeros(1,595); % speed vector
sv(1:595) = n;
SG = 1.033; % Spcific gravity of water
Hmax = 69.4; % Maximum head of pump (dead head)
```

```
bep = 0.875; % best efficiency point
Hbep = 47.5; % Pump head at best efficieny operating point
Qbep = 17000; %  Pump flow at best operating point
Qpump = 0:24000; % Individual pump flow rate vector
Hpumpspeed = ((nn/n).^2)*Hmax;
% Hpumpspeed = (((nn./n).^2)*Hmax)-(((nn./n).^2).*((Hmax-Hbep)*(((n./nn)*QQ)/Qbep).^2)); % Pump head at varying speed 0 to fullspeed 594RPM
% Hpump_red = (((nr/n)^2)*Hmax)-(((nr/n)^2)*((Hmax-Hbep)*(Qpump./Qbep).^2)); % Pump head/flow rate at desired speed
Hpump_red = (((nr/n)^2)*Hmax)-(((nr/n)^2)*((Hmax-Hbep)*(((n/nr)*Qpump)./Qbep).^2)); % Pump head/flow rate at desired speed
Hpump = Hmax-((Hmax-Hbep)*(Qpump/Qbep).^2); % Pump standard head/flow curve model
H = Hpump(QQ);
H2pump = zeros(1,48001); % combine 2 pump blank vector
H2pump_red = zeros(1,48001); %combine 2 pump blank vector for reduced speed
H2pump(1:24001)=Hmax; % set max head for 2 pumps at full speed
H2pump_red(1:24001)=55.042471289777690; % set max head for 2 pumps at reduced speed
H2pump(24001:48001)=Hpump; % combined pump curve at full speed
H2pump_red(24001:48001)=Hpump_red;  % combined pump curve at reduced speed
P90 = ((Q.^2) / ((KV90^2)*SG))*10.12; % Pressure drop with valve fully open
P60 = ((Q.^2) / ((KV60^2)*SG))*10.12; % Pressure drop with valve at 50 degrees
P50 = ((Q.^2) / ((KV50^2)*SG))*10.12; % Pressure drop with valve at 50 degrees
P30 = ((Q.^2) / ((KV30^2)*SG))*10.12; % Pressure drop with valve at 50 degrees
P40 = ((Q.^2) / ((KV40^2)*SG))*10.12; % Pressure drop with valve at 50 degrees
FCWPD = 10; % FCW pressure drop at rated flow in meters H2O
FCWQ1 = 1612; % FCW rated flow in m3/hr
CPPPD = 7.8; % CPP Condenser pressure drop at rated flow in meters H2O
CPPQ1 = 4726; % CPP Condenser rated flow in m3/hr
PD127 = 7.2; % 127MC pressure drop at rated flow in meters H2O
Q127 = 13335.25; % 127MC rated flow in m3/hr
MJTCPD = 7; % 127MC pressure drop at rated flow in meters H2O
MJTCQ1 = 13335.2; % 127MC rated flow in m3/hr
MJCCPD = 7; % 127MC pressure drop at rated flow in meters H2O
MJCCQ1 = Q127 - MJTCQ1; % 127MC rated flow in m3/hr
CPP_per = 0.2912; %CPP flow rate percentage
FCW_per = 0.2980; %CPP flow rate percentage
MC_per = 0.4108; %CPP flow rate percentage
Peff1 = 0.87;
Peff2 = 1-((1-(bep*(((2*(nr/n)*14183)/Qbep)-((((nr/n)*14183)^2)/(Qbep^2)))))*((nr/n)^0.1));
Peff = 1-((1-(bep*(((2*(n./nnr)*14183)/Qbep)-((((n./nnr)*14183).^2)./(Qbep^2))))).*((n./nnr).^0.1));
Pefftest = (1-((1-(bep*(((2*(nnr/n)*14183)/Qbep)-((((nnr/n)*14183).^2)./(Qbep^2))))).*((nnr/n).^0.1)))*100;
meff = 0.96;
```

```
Peff3 = 0.962;

Po1 = (365*2*24*150*QP*H1*1000*g)/(Peff1*meff*1000000*3600);
Po2 = (365*2*24*150*QP*H2*1000*g)/(Peff2*Peff3*meff*1000000*3600);
Po1I = (2*QP*H1*1000*g)/(Peff1*meff*1000000*3600);
Po2I = (2*QP*H2*1000*g)/(Peff3*Peff2*meff*1000000*3600);
Po2test = (365*2*24*150*QP*5.4756*1000*g)/(Peff3*Peff2*meff*1000000*3600);
Esaving = Po1-Po2;
%% CPP Friction %%
  %Series Path1%
D32_1= Hf(Q, 2.8, 32);     %S
D30_1= Hf(Q, 5.4, 30);     %S
D32_2= Hf(Q, 23.6, 32);    %S
D30_2= Hf(Q, 180.6, 30);   %S
D30_3= Hf(Q, 162.9, 30);   %S
D56_1= Hf(Q, 1.5, 56);     %S
S1 = D32_1+D30_1+D32_2+D30_2+D30_3+D56_1;
  %Parrallel Path 1%
D30_4= Hf(Q, 11.8, 30);    %S
D30_5= Hf(Q, 1.54, 30);    %P1
D24_1= Hf(Q, 3.95, 24);    %P1
D24_2= Hf(Q, 3.97, 24);    %P2
CPPF1 = QF(Q, CPPQ1, CPPPD); %CPP Friction
D24_3= Hf(Q, 11.5, 24);    %P3
D24_4= Hf(Q, 11.2, 24);    %P4
D30_6= Hf(Q, 4.2, 30);     %P4
D30_7= Hf(Q, 8.5, 30);     %S
CPP1 =
D30_4+D30_7+CPPF1+(1./(1./D30_5+D24_1)+1./(1./D24_1))+(1./(1./D30_6+D24_4)+1./(1./
D24_3));

%Parrallel Path 2%
D30_8= Hf(Q, 25, 30);     %S
D30_9= Hf(Q, 1.52, 30);    %P1
D24_5= Hf(Q, 2.45, 24);    %P1
D24_6= Hf(Q, 2.8, 24);    %P2
%CPP2 series%             %S
D24_7= Hf(Q, 11.5, 24);    %P3
D24_8= Hf(Q, 11.2, 24);    %P4
D30_10= Hf(Q, 4.2, 30);     %P4
D30_11= Hf(Q, 31, 30);     %S
CPP2 =
D30_8+D30_11+CPPF1+(1./(1./D30_9+D24_5)+1./(1./D24_6))+(1./(1./D30_10+D24_8)+1./(1
./D24_7));

  %Series Path2%
D30_12= Hf(Q, 162.9, 30);     %S
```

```
D56_2= Hf(Q, 3, 56);      %S
S2 = D30_12+D56_2;

CPPFriction = CPP_per*(S1+S2+ 1./((1./CPP1)+(1./CPP2)));

%% FCW Exchanger %%
   %Series Path1%
D72_F1 = Hf(Q, 3.43, 72);      %S
D42_F1 = Hf(Q, 10.47, 42);      %S
D40_F1 = Hf(Q, 27.67, 40);      %S
D68_F1 = Hf(Q, 16.74, 68);      %S
S3 = D72_F1+D42_F1+D40_F1+D68_F1;
   %Parrallel Path1%
D40_F2 = Hf(Q, 2.9, 40);      %P
D12_F1 = Hf(Q, 7.69, 12);      %P
D68_F3 = Hf(Q, 2.9, 68);      %P
FCWF1 = QF(Q, FCWQ1, FCWPD);
%FCWEXchanger
FCW = (D40_F2+D12_F1+D68_F3+FCWF1)/6;

FCWFriction = FCW_per*(FCW+S3);

%% 127MC %%
   %Series Path1%
D72_M1 = Hf(Q, 1.56, 72);              %S
D48_M1 = Hf(Q, 159, 48);               %S
D56_M1 = Hf(Q, 3, 56);                 %S
F127MC = QF(Q, Q127, PD127); % 127MC friction
SM1 = D72_M1+D48_M1+D56_M1+F127MC;
%SM1 = D72_M1+D48_M1+D56_M1;
   %Parrallel Path1%
D6_M1 = Hf(Q, 81.722, 6);              %P1
MJCCF = QF(Q, MJCCQ1, MJCCPD); %103MJCC   %P1
D48_M2 = Hf(Q, 33.4, 48);              %P2
MJTCF = QF(Q, MJTCQ1, MJTCPD); %103MJTC   %P2
%PM1 = 1./((1./(D6_M1))+(1./(D48_M2)));
PM1 = 1./((1./(D6_M1+MJCCF))+(1./(D48_M2+MJTCF)));

MCFriction = MC_per*(PM1+SM1);


%% Pump Friction %%
   %Series 1%
D42_P1 = Hf(Q, 12.4, 42);        %S1
D48_P1 = Hf(Q, 37.74, 48);        %S1
MOV2401_90 = P90;
MOV2401_60 = P60;
```

```
MOV2401_50 = P50;
MOV2401_30 = P30;
MOV2401_40 = P40;
D72_P1 = Hf(Q, 67.54, 72);         %S1

PumpFriction90 =  0.5*(D42_P1+D48_P1+MOV2401_90+D72_P1);
PumpFriction50 =  0.5*(D42_P1+D48_P1+MOV2401_50+D72_P1);
PumpFriction0 =  0.5*(D42_P1+D48_P1+D72_P1);

%% Cooling Tower Friction %%
D68_C1 = Hf(Q, 39.9, 68);         %P1
D56_C1 = Hf(Q, 94.7, 56);         %P1
D68_C2 = (Hf(Q, 40.251, 68))/2;         %S1

CTFriction = D68_C2 + 1./((1./D68_C1)+(1./D56_C1));

TotalFriction90 = CTFriction +PumpFriction90+ 1./((1./MCFriction)+(1./FCWFriction)...
    +(1./CPPFriction));
TotalFriction50 = CTFriction +PumpFriction50+ 1./((1./MCFriction)+(1./FCWFriction)...
    +(1./CPPFriction));
TotalFriction0 = CTFriction +PumpFriction0+ 1./((1./MCFriction)+(1./FCWFriction)...
    +(1./CPPFriction));
TotalHead90 = TotalFriction90+30;
TotalHead50 = TotalFriction50+30;
TotalHead0 = TotalFriction0+30;
NVH = (TotalHead90(28366))-(TotalHead0(28366));
ENVH = (365*2*24*150*QP*NVH*1000*g)/(Peff2*Peff3*meff*1000000*3600);
figure(1);
plot(Q,TotalHead0);
hold on
plot(Q,TotalHead50);
%plot(Q,TotalHead0);
plot(Q1, Hpump);
plot(Q1, Hpump_red);
xlim([0,48000]);
ylim([0,120]);
title('Pump & System Curve');
xlabel('Flow Rate (m3hr)')
ylabel('Total Head (m)')
legend({'y1 = Valve Removed','y2 = Valve actual position','y3 = Pump Curve @ 594RPM','y4 =
Pump Curve @ 569RPM'},...
'Location','southwest')
hold off

figure(2);
plot(nn,Hpumpspeed);
%xlim([0,48000]);
```

```
%ylim([0,120]);
title('Pump Head at Varying Speed');
xlabel('Pump Speed (RPM)')
ylabel('Pump Head (m)')

figure(3);
plot(Q,TotalHead50);
xlim([0,48000]);
ylim([0,100]);
title('Hydraulic System Curve');
xlabel('Flow Rate (m3h)')
ylabel('Pump Head (m)')

figure(4);
plot(Q1, Hpump);
xlim([0,48000]);
ylim([0,100]);
title('Pump Curve');
xlabel('Flow Rate (m3hr)')
ylabel('Total Head (m)')

figure(5);
plot(nnr, Pefftest);
xlim([0,594]);
ylim([0,100]);
title('Pump Efficiency Curve');
xlabel('Pump Speed (RPM)')
ylabel('Pump Efficiency (%)')

figure(6);
%plot(Q,TotalHead90);
plot(Q,TotalHead50);
hold on
plot(Q1, Hpump);
%plot(Q1, Hpump_red);
xlim([0,48000]);
ylim([0,120]);
title('Pump & System Curve');
xlabel('Flow Rate (m3hr)')
ylabel('Total Head (m)')
legend({'y1 = Valve 50 degrees','y2 = Pump Curve @ 594RPM'},...
'Location','southwest')
hold off

figure(7);
plot(Q,TotalHead90);
hold on
```

```
plot(Q,TotalHead50);
plot(Q1, Hpump);
%plot(Q1, Hpump_red);
xlim([0,48000]);
ylim([0,120]);
title('Pump & System Curve');
xlabel('Flow Rate (m3hr)')
ylabel('Total Head (m)')
legend({'y1 = Valve 90 degrees','y2 = Valve actual position','y3 = Pump Curve @ 594RPM'},...
'Location','southwest')
hold off

% Function definition
function friction = Hf(Q, L, D)
friction = (10.67*(Q/(3600*150)).^1.85)*((L)/((D*0.0254)^4.87));
end

function Qfriction = QF(Q,Q1,HF1)
Qfriction = ((Q/Q1).^2)*HF1;
end
```

Appendix L

Piping Isometrics Example

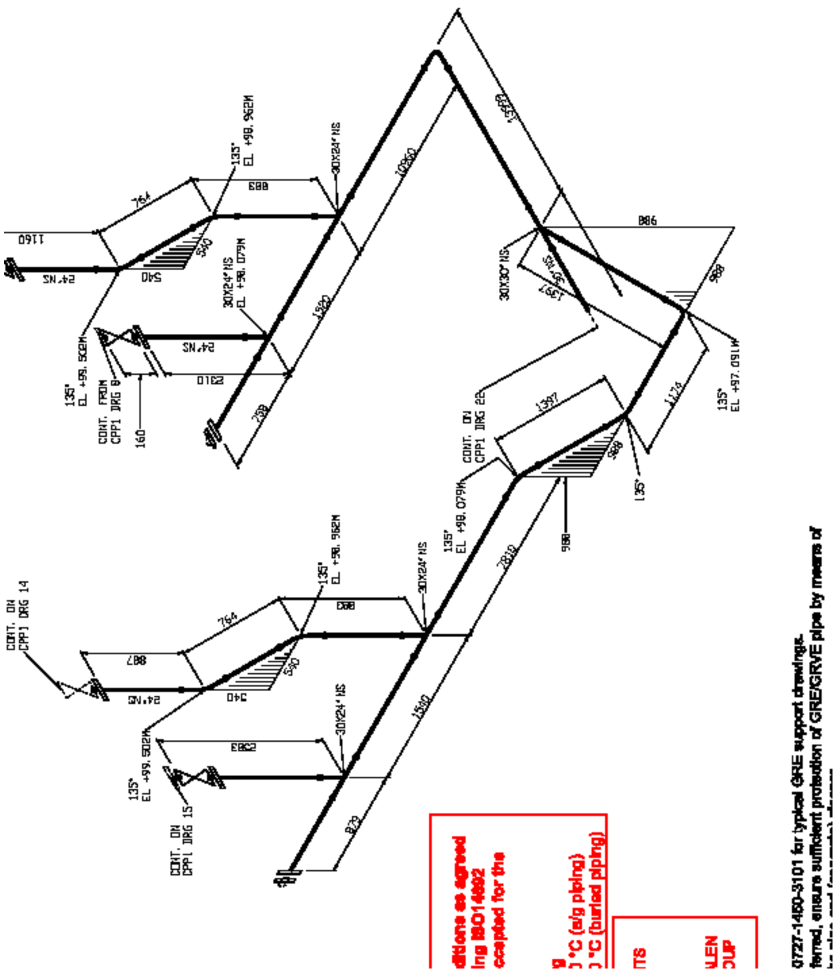

Appendix M

Installation Costs

We have pleasure in submitting our budget estimate for works associated with the above project.

Price	$ 43,500.00 each x 3 Total $ 130,500.00
Plus 10% GST	$ 13,050.00
Total Including GST	**$ 143,550.00**

The above price is valid for 30 (Thirty) days from the date of this quotation. Please refer to the attached Terms & Condition for terms of payment. Price is subject to our standard terms and conditions.

Scope of Works:

1. Conduct risk assessment and obtain HV access permit and permit to work.
2. Disconnection, removal, and disposal of existing HV soft starter.
3. Transport VSD into Sea cooling water substation.
4. Relocation of LV switchboard currently mount on back of soft starter panel to the wall beside fire panel.
5. Installation and connection of VSD.
6. Allowance of 50m of 6.6kv 185mm SWA cable for connection from switchgear to new VSD panel if required.
7. Modification of interconnection control wiring.
8. Testing and commissioning, with an allowance of $10,000 for ABB tech one visit 3 VSD's.
9. Provide testing certificates, ITR's, notice of completion and logbook entry.
10. Provide as-built documentation

Excluded:

1. Site amenities.
2. Supply of VSD panels.
3. Supply of crane, operator, and rigger.
4. Extension of field motor cabling if needed.

We have assumed that the new panels will fit through the existing door opening and room available through the sub stations.

Appendix N

Condenser Datasheet Example

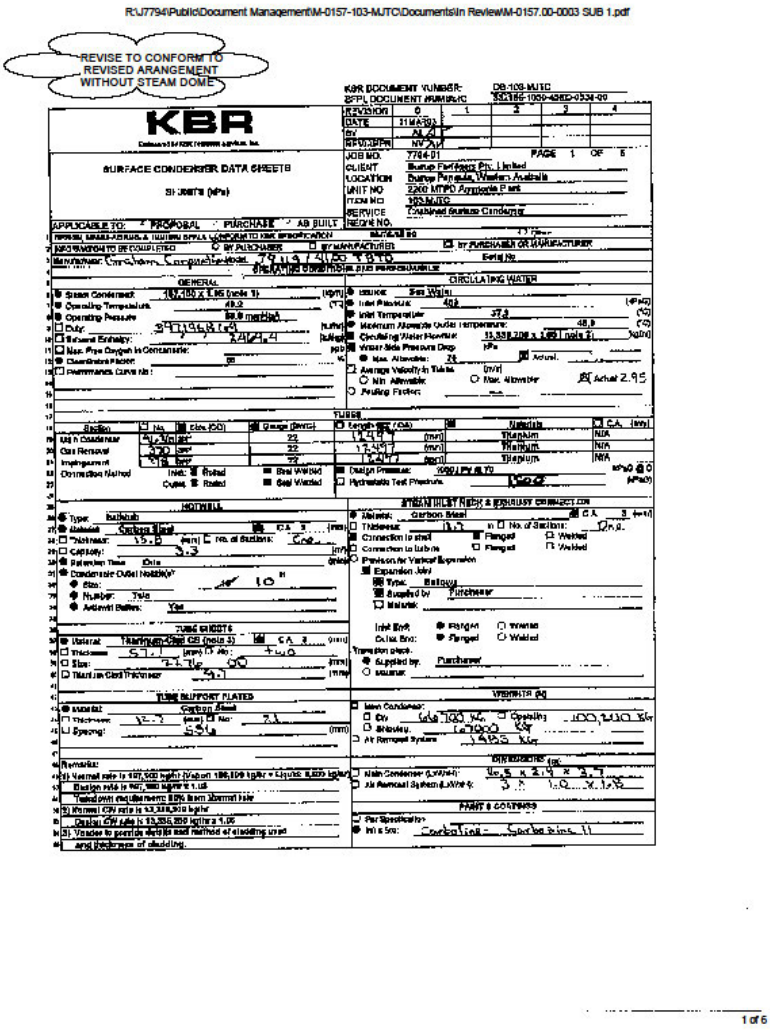
R:\J7794\Public\Document Management\M-0157-103-MJTC\Documents\In Review\M-0157.00-0003 SUB 1.pdf

REVISE TO CONFORM TO
REVISED ARANGEMENT
WITHOUT STEAM DOME

KBR

SURFACE CONDENSER DATA SHEETS

APPLICABLE TO: PROPOSAL PURCHASE AS BUILT

REVISION 0 1 2 3 4

PAGE 1 OF 5

GENERAL

CIRCULATING WATER

TUBES

Section

Main Condenser

Gas Removal

Impingement

Connection Method

Titanium

N/A

HOTWELL

STEAM INLET NECK & EXHAUST CONNECTION

Carbon Steel

Expansion Joint

Bellows

Purchaser

TUBE SHEETS

TUBE SUPPORT PLATES

Carbon Steel

WEIGHTS

DIMENSIONS

PAINT & COATINGS

Remarks:

1 of 6

Appendix O

Exchanger Datasheet Example

SPECIFICATION SHEET
SHELL AND TUBE EXCHANGER

KBR
Engineered by KBR Technical Services, Inc.

Form EXCHST01 (07/98) (SI Units)

REVISION	0		1		2		3	
NUMBER	By	Date	By	Date	By	Date	By	Date
Originator	RLC	26Mar03	RLC	02Apr03				
Check	ACM	26Mar03	ACM	02Apr03				
Approved	ACM	26Mar03	ACM	02Apr03				
Issued	26Mar03		02Apr03					

Job No.	J7794	Page 1 of 4	
Client	BURRUP FERTILISERS PTY LTD		
Location	KARRATHA, WESTERN AUSTRALIA		
Item No.	127-MC		
Process Unit	2200 MTPD AMMONIA PLANT		
Document No.	MC3A-127MC		
Client Document No.	332186-1040-45ED-0219-00		

1	Service of Unit	REFRIGERANT CONDENSER; No. of Units 1
2	Size	2150-8500; Type AJL (Horizontal); Connected in 1 Parallel 1 Series
3	Surface/Unit (Eff.)	2856 m²; Shells/Unit 1; Surface/Shell (Eff.) 2856 m²
4	PERFORMANCE OF ONE UNIT	

	5	Fluid Allocation		SHELL SIDE				TUBE SIDE			
	6	Fluid Name		AMMONIA				SEA WATER			
[1]	7	Fluid Quantity, Total	kg/hr	124199 x 1.05				13335250 x 1.05			
	8	Vapor (In/Out)	kg/hr	124199 x 1.05		1946 x 1.05		-		-	
	9	Liquid	kg/hr	-		122253 x 1.05		-		-	
	10	Steam	kg/hr	-		-		-		-	
[1]	11	Water	kg/hr	-		-		13335250 x 1.05		13335250 x 1.05	
	12	Noncondensable (MW)	kg/hr	-		-					
	13	Temperature (In/Out)	°C	112.6		43.8		35.0		37.9	
	14	Density (Vapor/Liquid)	kg/m³	10.53		13.38	573.83	-	1033.	-	-
	15	Viscosity (Vapor/Liquid)	cP	0.01		0.01	0.12	-	-	-	-
	16	Molecular Weight, Vapor		17.03		16.92		-		-	
	17	Specific Heat (Vapor/Liquid)	kJ/kg °C	2.62		2.902	4.896	-	4.	-	-
	18	Thermal Conductivity (Vapor/Liquid)	W/m °C	0.036		0.029	0.436	-	-	-	-
	19										
	20										
	21	Latent Heat	kJ/kg	SEE HEAT RELEASE CURVE, PAGE 2				-			
	22	Inlet Pressure	kPa (ABS)	1821.							
	23	Velocity	m/s					2.78			
	24	Pressure Drop (Allowable/Calculated)	kPa	25.		12.		75.		72.	
	25	Fouling Resistance (Min.)	m² °C/W	0.00009				0.00018			

26	Heat Exchanged	154.92 x 1.05 GJ / hr; MTD (Corrected) (Weighted) 10.0 °C
27	Transfer Rate (Service/Clean)	1592 W/m² °C
28	CONSTRUCTION OF ONE SHELL	

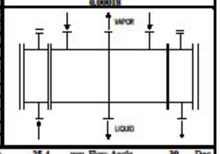

				Shell Side	Tube Side
29				SHELL SIDE	TUBE SIDE
30	Design Pressure/Vacuum Pressure		kPa g	2000 /	1000 / FV
31	Design Temperature (Max/Min)		°C	150 / 10	100 / 10
32	Corrosion Allowance		mm	1.5	NONE
33	No. of Passes per Shell			1	1
34	Connections Size & Rating	In		2 x 16"-300# RF	48-150# RF
35		Out		12"-300# RF (LIQ)	48-150# RF
36				3"-300# RF (VAP)	2 x 1"-150# RF (7)

37	Tube No. 5856 OD 19.05 mm Thk 0.89 mm (Avg.)	Length 8500 mm Pitch 25.4 mm Flow Angle 30 Deg.
38	Tube Type STRAIGHT	Material TITANIUM
39	Shell C.S. ID 2150 OD - mm	Shell Cover -
40	Channel or Bonnet SOLID TITANIUM OR TITANIUM-CLAD C.S.	Channel Cover SOLID TITANIUM OR TITANIUM-CLAD C.S.
41	Tubesheet - Stationary TITANIUM-CLAD C.S.	Tubesheet - Floating -
42	Floating Head Cover -	Impingement Protection YES, C.S. PLATE
43	Baffles - Cross C.S. Type VERTICAL DBL. SEG. (1) (2) (3) No. Crosspasses 20	% Cut 47.5 (Area) Central Spacing 401 (5) mm
44	Baffles - Long -	Seal Type -
45	Supports - Tube C.S.	Type (4)
46	Bypass Seal Arrangement C.S., 1-PAIR SEAL STRIPS	Tube - Tubesheet Joint NO GROOVES, EXPAND & SEAL WELD
47	Expansion Joint C.S., FLANGED & FLUED IF REQUIRED	Metal Temp. for Expansion (Shell/Tube) 51 / 42 °C
48	Gaskets - Shell Side - Tube Side FLEXIBLE GRAPHITE	Floating Head -
49	Code Requirements ASME SECT. VIII DIV. 1	Stamp YES TEMA Class "R"
50	REMARKS:	
51	1) INLET AND OUTLET BAFFLES TO BE 'ONE-PIECE' TYPE. INLET BAFFLES TO BE PROVIDED WITH EARS ON THE TOP	
52	TO SUPPORT A MINIMUM OF 35 TUBE ROWS.	
53	2) ONE-PIECE BAFFLES TO BE PROVIDED WITH A 25 MM NOTCH ON THE BOTTOM FOR DRAINAGE.	
54	3) BAFFLES TO BE PROVIDED WITH EARS ON THE TOP TO PREVENT VAPOR BY-PASSING.	
55	4) PROVIDE A FULL SUPPORT PLATE AT THE SHELLSIDE OUTLET NOZZLES. PROVIDE A PARTIAL TUBE SUPPORT AT	
56	THE SHELLSIDE INLET NOZZLES TO SUPPORT A MINIMUM OF 35 TUBE ROWS.	
57	5) INLET BAFFLE SPACE TO BE APPROX 660 MM.	
58	6) EXCHANGER IS ELEVATED ABOVE THE REFRIGERANT DRUM. PROVIDE GRAVITY FLOW FROM 127-MC TO REFRIGERANT DRUM.	
59	7) PROVIDE A 1"-150# RF VENT WITH BLIND ON EACH CHANNEL.	
60		
61		

S:\Engr\Exchangers\Exch-General\Work\AmmJob\J7794 Burrup\Issued Deliverables\Specification Sheets\Final Issue\[MC3A-127MC.xls]

Appendix P

Purchase Costs

Option	Datasheet	Budget Price Each	Budget Price Total
ACS580MV (If motors are suitable for VSD)	DS44696-01	$261,000.00	$783,000.00
ACS2000 (Fitted with Sine filter for non-VSD motor)	DS44696-02	$375,000.00	$1,125,000.00

Appendix Q

Simscape Model

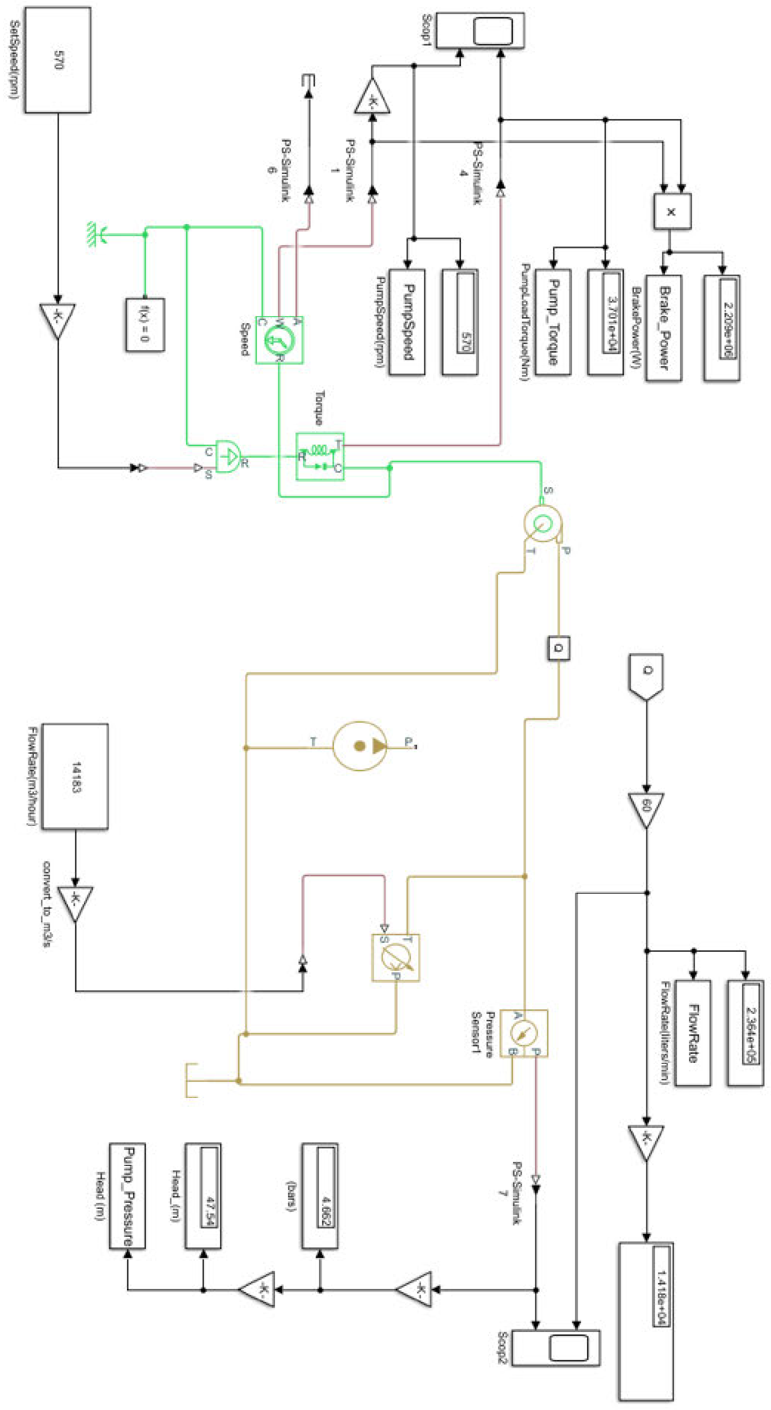

(Page Left Intentionally Blank)